Quasibound states in short SNS junctions with point defects

A. A. Bespalov
Institute for Physics of Microstructures, Russian Academy of Sciences, 603950 Nizhny Novgorod, GSP-105, Russia

(Received 13 February 2018; published 6 April 2018)

Using the Green functions technique, we study the subgap spectrum of short three-dimensional superconductor–normal metal–superconductor junctions containing one or two point impurities in the normal layer. We find that a single nonmagnetic or magnetic defect induces two quasibound Shiba-like states. If the defect is located close to the junction edge, the energies of these states oscillate as functions of the distance between the impurity and the edge. In the case of two nonmagnetic impurities, there are generally four quasibound states (two per spin projection). Their energies oscillate as functions of the distance between the impurities, and reach their asymptotic values when this distance becomes much larger than the Fermi wavelength. The contributions of the impurities to the Josephson current, local density of states, and to the normal-state conductance of the junction are analyzed.

DOI: 10.1103/PhysRevB.97.134504

I. INTRODUCTION

The effect of disorder on the superconducting correlations has been studied for several decades starting from the seminal papers by Anderson [1] and Abrikosov and Gor'kov [2]. In many experiments the measurable quantities such as the critical temperature, electromagnetic response, and the density of states are well determined by their values averaged over disorder. Still there exists a number of important experimental situations when the averaged quantities do not give us the information needed for the understanding the properties of a particular sample. In this case we often need to focus on the properties of an individual impurity or defect and develop an appropriate theoretical description providing the information necessary for the experiment interpretation. One can enumerate the following research directions for which the consideration of an individual impurity is crucial. First, the study of the local electronic characteristics around the individual impurity can help to identify the type of superconducting pairing. Indeed, the scattering process mixes different quasiparticle momenta and the resulting impurity states are sensitive to the momentum dependence of the superconducting order parameter [3]. Thus the impurity atom serves in some sense as a probe of the order parameter symmetry. Second, the solution of the scattering problem for a few impurities becomes necessary for rather small samples, i.e., at so-called mesoscopic length scales. In this regime the transport characteristics strongly fluctuate from sample to sample and the calculations of ensemble averages can be irrelevant [4]. To sum up, individual impurities are known to produce well-observable local modifications of the electronic structure in normal and superconducting metals, including spatial oscillations of the density of states [5] and localized subgap states in superconductors with conventional [6–8] and unconventional pairing (see Ref. [3] for review).

It should be also noted that the consideration of the problem with an individual impurity or a few of them allows often to get a deeper insight into the physics of processes which occur in large impurity ensembles. To give just a simple example one can recall the Larkin-Ovchinnikov solution [9] for the electronic structure of the superconducting vortex with a single impurity atom in the core which allowed one to understand the Landau-Zener mechanism of dissipation accompanying the vortex motion [9–11]. In this sense the present paper continues the series of works studying the effect of individual impurities on the inhomogeneous superconducting states and focuses on the analysis of the defects in a Josephson junction with a certain nonzero phase difference between the superconducting leads.

Quite naturally the effect of impurities strongly depends on the system dimensionality. The simplest one-dimensional (1D) limit when the nonmagnetic defects can be described by certain potential barriers has been previously considered in a large number of papers (see Refs. [12,13] for review, and also Refs. [14–16]). The same can be said about the case of magnetic scatterers/barriers [12,13,17–21]. It is a more complicated task to analyze substantially 3D systems, e.g., impurities in bulk materials or wide wires. Indeed, little is known about the influence of individual impurities on inhomogeneous superconducting systems. Covaci *et al.* [22,23] developed an efficient numerical algorithm to solve the Bogoliubov–de Gennes equations self-consistently, and applied this method to calculate the local density of states and Josephson current in 2D SNS junctions with disorder. Avotina *et al.* [24] have studied mesoscopic conductance fluctuations of a SN tunnel junction with a point impurity. Omelyanchouk *et al.* [25] have calculated the stationary current in a Josephson junction with point impurities located in an orifice between the superconducting banks. In this work we present a general approach, which allows one to study the electronic structure of inhomogeneous superconducting systems with one or several point impurities. In particular, we provide an explicit method to calculate the Green functions of a system with defects using only the Green function of a pure system.

The main result of the paper is the discovery of a quasibound subgap state at a nonmagnetic impurity located inside the normal layer of a SNS Josephson junction with a nonzero phase difference φ between the superconducting leads. This state is somewhat similar to the Yu-Shiba-Rusinov state [6–8] induced by a magnetic impurity in a homogeneous superconductor. In an infinite junction the impurity state appears within the

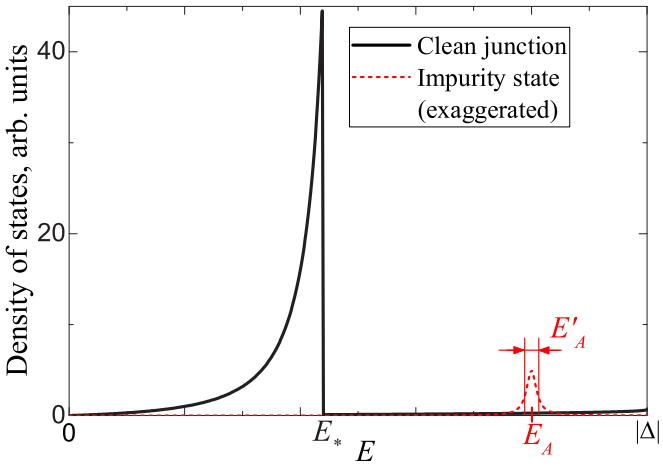

FIG. 1. Subgap density of states of a short, but infinitely wide SNS junction with a nonmagnetic point impurity. The spectrum of a clean junction [26], shown as a solid line, has a sharp peak at an energy $E_* \approx |\Delta|\cos(\varphi/2)$, where $|\Delta|$ is the gap in the superconducting banks. At energies higher than E_* there is still a nonzero density of states, and in this region the impurity state appears (dashed line, shown strongly exaggerated).

continuous subgap spectrum of the system (see Fig. 1), and thus it has a complex energy: $E = E_A - iE'_A$, such that $E'_A/\hbar$ is the decay rate of the state. In a finite sized junction all subgap states are localized and the spectrum is discrete. The impurity state is a superposition Andreev states of the pure junction, whose energies are located in a window around E_A with a width E'_A. This means that, as long as the distance between these energy levels is much smaller than E'_A, the spatial structure and the decay rate of the impurity state are almost not modified.

We analyze the behavior of the impurity states when the defect (either nonmagnetic or magnetic) is located close to the surface of a semi-infinite junction. We find the oscillations of the energies of the impurity states as functions of the distance between the defect and the sample surface. Finally, for two nonmagnetic impurities inside the normal region we find two quasibound states (per spin projection), whose energies strongly depend on the relative positions of the defects.

The structure of the paper is as follows. In Sec. II our technique of calculating the Green functions in SN systems with a point impurity is described. We show how the Green functions of a system with and without defects are related to each other. In Sec. III we analyze a short SNS junction with one nonmagnetic or magnetic impurity. The Green functions and the energies of the impurity states are calculated and the influence of the sample surface on these states is considered. Section IV is devoted to SNS junctions with two nonmagnetic impurities. Here, we concentrate on the energies of the localized states only. In Sec. V we discuss how individual defects influence such measurable characteristics as the Josephson current and normal-state conductance of the junction. In the conclusion the main results are summarized.

II. BASIC EQUATIONS

Within the mean-field approach, a nonuniform superconducting system with a point impurity can be characterized by the Hamiltonian

$$\mathcal{H} = \sum_{\alpha\beta}\int \psi^\dagger_\alpha(\mathbf{r})[H_0(\mathbf{r})\delta_{\alpha\beta} + V_{\alpha\beta}(\mathbf{r}-\mathbf{r}_1)]\psi_\beta(\mathbf{r})d^3\mathbf{r} + \int[\Delta^*(\mathbf{r})\psi_\uparrow(\mathbf{r})\psi_\downarrow(\mathbf{r}) + \Delta(\mathbf{r})\psi^\dagger_\downarrow(\mathbf{r})\psi^\dagger_\uparrow(\mathbf{r})]d^3\mathbf{r}. \quad (1)$$

Here, $\psi^\dagger_\alpha$ and ψ_α are the electron creation and annihilation operators, respectively ($\alpha,\beta = \uparrow,\downarrow$ are the spin indices),

$$H_0(\mathbf{r}) = -\frac{\hbar^2\nabla^2}{2m} - \mu, \quad (2)$$

where m is the electron mass and μ is the chemical potential, $\Delta(\mathbf{r})$ is the superconducting order parameter, and the matrix impurity potential $V_{\alpha\beta}$ is given by

$$\hat{V}(\mathbf{r}) = U(\mathbf{r})\hat{\sigma}_0 + \mathbf{J}(\mathbf{r})\hat{\boldsymbol{\sigma}}, \quad (3)$$

where $U(\mathbf{r})$ is an electric potential, $\mathbf{J}(\mathbf{r})$ is an exchange field, $\hat{\sigma}_0$ is a unit matrix, and $\hat{\boldsymbol{\sigma}}$ are the Pauli matrices.

We will concern ourselves only with the retarded Green function $\check{G}_E(\mathbf{r},\mathbf{r}')$ of the system—this function contains all the information about single-particle characteristics, such as the current density and the local density of states. The Green function satisfies the Gor'kov equation [27]:

$$\left\{\hat{\tau}_0[H_0(\mathbf{r}) + U(\mathbf{r}-\mathbf{r}_1)] + \hat{\tau}_z[\mathbf{J}(\mathbf{r}-\mathbf{r}_1)\hat{\boldsymbol{\sigma}} - E - i\epsilon^+] + \begin{pmatrix} 0 & -\Delta(\mathbf{r}) \\ \Delta^*(\mathbf{r}) & 0 \end{pmatrix}\right\}\check{G}_E(\mathbf{r},\mathbf{r}') = \hat{\tau}_0\delta(\mathbf{r}-\mathbf{r}'). \quad (4)$$

Here, $\hat{\tau}_0$ and $\hat{\tau}_z$ are a unit and a Pauli matrix in Nambu space, respectively, E is the energy, and ϵ^+ is an infinitely small positive quantity. The 4×4 matrix $\check{G}_E$ has the following block structure:

$$\check{G}_E(\mathbf{r},\mathbf{r}') = \begin{pmatrix} \hat{G}_E(\mathbf{r},\mathbf{r}') & \hat{F}_E(\mathbf{r},\mathbf{r}') \\ -\hat{F}^\dagger_E(\mathbf{r},\mathbf{r}') & \hat{\bar{G}}_E(\mathbf{r},\mathbf{r}') \end{pmatrix}. \quad (5)$$

For the definition of the 2×2 blocks in terms of the electron field operators the reader may refer to Appendix A. Now, we can explicitly write down the local density of states $\nu(E,\mathbf{r})$:

$$\nu(E,\mathbf{r}) = \pi^{-1}\mathrm{Im}[G_{E\uparrow\uparrow}(\mathbf{r},\mathbf{r}) + G_{E\downarrow\downarrow}(\mathbf{r},\mathbf{r})]. \quad (6)$$

Our strategy for solving Eq. (4) is to relate $\check{G}_E(\mathbf{r},\mathbf{r}')$ to the Green function $\check{G}^{(0)}_E(\mathbf{r},\mathbf{r}')$ of the superconductor without the impurity, i.e., with $\hat{V}(\mathbf{r}) = 0$. The latter Green function can be then determined using well-developed quasiclassical methods (see below).

Speaking about the point impurity, we imply that the range of its potential $V(\mathbf{r})$ is much smaller than the Fermi wavelength. Then, it is a predominantly isotropic scatterer, i.e., an effective source of spherical waves. In this sense, it acts similar to the δ-function source in the right-hand side of Eq. (4). Given this, we seek the solution of Eq. (4) in the form

$$\check{G}_E(\mathbf{r},\mathbf{r}') = \check{G}^{(0)}_E(\mathbf{r},\mathbf{r}') + \check{G}^{(0)}_E(\mathbf{r},\mathbf{r}_1)\check{A}(\mathbf{r}_1,\mathbf{r}'), \quad (7)$$

where $\check{A}(\mathbf{r}_1,\mathbf{r}')$ is an unknown matrix, which is defined by the behavior of $\check{G}^{(0)}_E(\mathbf{r},\mathbf{r}')$ in the vicinity of the impurity, i.e., $\mathbf{r}\approx\mathbf{r}_1$. The problem of calculating $\check{A}(\mathbf{r}_1,\mathbf{r}')$ is relatively simply

solved in 1D, where we can put

$$\hat{V}(\mathbf{r}) = (U\hat{\sigma}_0 + \mathbf{J}\hat{\boldsymbol{\sigma}})\delta(\mathbf{r}) \tag{8}$$

and determine the Green function from a Dyson equation, as described in Ref. [14]. Such a solution is possible because $\check{G}_E^{(0)}(\mathbf{r}_1,\mathbf{r}_1)$ is finite in 1D; however, this is not the case in higher dimensions. In Appendix B we illustrate how to calculate $\check{A}(\mathbf{r}_1,\mathbf{r}')$ by a simpler example of a nonmagnetic and nonsuperconducting system. In short, the procedure consists in separating in Eq. (7) the regular part of $\check{G}_E(\mathbf{r},\mathbf{r}')$ at $\mathbf{r}=\mathbf{r}_1$ and the $\propto|\mathbf{r}-\mathbf{r}_1|^{-1}$ singularity. Then, using basic scattering theory, a relation between these parts can be obtained [see Eq. (B7)]. This generally yields 16 coupled linear algebraic equations for the components of $\check{A}(\mathbf{r}_1,\mathbf{r}')$. The situation is significantly simplified in our case, since we are dealing with one impurity in a nonmagnetic environment. Then, the Green function of the pure system is proportional to the unit matrix in spin space: $\hat{G}_E^{(0)} = G_E^{(0)}\hat{\sigma}_0$, $\hat{F}_E^{(0)} = F_E^{(0)}\hat{\sigma}_0$, $\hat{\bar{G}}_E^{(0)} = \bar{G}_E^{(0)}\hat{\sigma}_0$, and $\hat{F}_E^{\dagger(0)} = F_E^{\dagger(0)}\hat{\sigma}_0$. For brevity, we introduce the notation

$$\hat{G}_E^{(0)}(\mathbf{r},\mathbf{r}') = \begin{pmatrix} G_E^{(0)}(\mathbf{r},\mathbf{r}') & F_E^{(0)}(\mathbf{r},\mathbf{r}') \\ -F_E^{\dagger(0)}(\mathbf{r},\mathbf{r}') & \bar{G}_E^{(0)}(\mathbf{r},\mathbf{r}') \end{pmatrix}. \tag{9}$$

If we direct the spin quantization axis along the impurity spin [parallel to $\mathbf{J}(\mathbf{r})$], the components of $\check{G}_E(\mathbf{r},\mathbf{r}')$ with spin indices $\uparrow\downarrow$ and $\downarrow\uparrow$ vanish, and the equations for the components with indices $\uparrow\uparrow$ and $\downarrow\downarrow$ decouple. For spin "up" components Eq. (7) takes the form

$$\begin{pmatrix} G_{E\uparrow\uparrow}(\mathbf{r},\mathbf{r}') & F_{E\uparrow\uparrow}(\mathbf{r},\mathbf{r}') \\ -F^{\dagger}_{E\uparrow\uparrow}(\mathbf{r},\mathbf{r}') & \bar{G}_{E\uparrow\uparrow}(\mathbf{r},\mathbf{r}') \end{pmatrix} = \hat{G}_E^{(0)}(\mathbf{r},\mathbf{r}') + \hat{G}_E^{(0)}(\mathbf{r},\mathbf{r}_1)\begin{pmatrix} A_{1\uparrow}(\mathbf{r}_1,\mathbf{r}') & A_{3\uparrow}(\mathbf{r}_1,\mathbf{r}') \\ A_{2\uparrow}(\mathbf{r}_1,\mathbf{r}') & A_{4\uparrow}(\mathbf{r}_1,\mathbf{r}') \end{pmatrix}. \tag{10}$$

When writing down conditions of the form (B7) for the Green functions, it should be born in mind that the pairs of functions $G_{E\uparrow\uparrow}$, $F_{E\uparrow\uparrow}$ and $\bar{G}_{E\uparrow\uparrow}$, $F^{\dagger}_{E\uparrow\uparrow}$ "feel" different scattering potentials, because the exchange term appears with opposite signs for these pairs in Eq. (4). Thus the impurity produces a scattering phase $\alpha_\uparrow$ for $G_{E\uparrow\uparrow}$ and $F_{E\uparrow\uparrow}$ and a scattering phase $\alpha_\downarrow$ for $\bar{G}_{E\uparrow\uparrow}$ and $F^{\dagger}_{E\uparrow\uparrow}$. Applying the expansion (B7) to $G_{E\uparrow\uparrow}(\mathbf{r},\mathbf{r}')$ and $F^{\dagger}_{E\uparrow\uparrow}(\mathbf{r},\mathbf{r}')$ near $\mathbf{r}=\mathbf{r}_1$, we obtain the relations

$$\frac{mA_{1\uparrow}}{2\pi\hbar^2} = \frac{\tan\alpha_\uparrow}{k_F}\big[G_E^{(0)}(\mathbf{r}_1,\mathbf{r}') + A_{1\uparrow}G_{ER}^{(0)}(\mathbf{r}_1,\mathbf{r}_1) + A_{2\uparrow}F_E^{(0)}(\mathbf{r}_1,\mathbf{r}_1)\big], \tag{11}$$

$$-\frac{mA_{2\uparrow}}{2\pi\hbar^2} = \frac{\tan\alpha_\downarrow}{k_F}\big[F_E^{\dagger(0)}(\mathbf{r}_1,\mathbf{r}') + A_{1\uparrow}F_E^{\dagger(0)}(\mathbf{r}_1,\mathbf{r}_1) - A_{2\uparrow}\bar{G}_{ER}^{(0)}(\mathbf{r}_1,\mathbf{r}_1)\big], \tag{12}$$

where $k_F = (2m\mu/\hbar^2)^{1/2}$ is the Fermi wave number. When writing down the solution of the linear Eqs. (11) and (12), we will use the relations $\bar{G}_E^{(0)} = G_{-E}^{(0)*}$ and $F_E^{(0)} = F_{-E}^{\dagger(0)*}$ [these follow from Eq. (4)]:

$$A_{1\uparrow}(\mathbf{r}_1,\mathbf{r}') = \mathcal{D}_\uparrow^{-1}\left\{G_E^{(0)}(\mathbf{r}_1,\mathbf{r}')\left[\frac{mk_F\cot\alpha_\downarrow}{2\pi\hbar^2} - G_{-ER}^{(0)*}(\mathbf{r}_1,\mathbf{r}_1)\right] - F_{-E}^{\dagger(0)*}(\mathbf{r}_1,\mathbf{r}_1)F_E^{\dagger(0)}(\mathbf{r}_1,\mathbf{r}')\right\}, \tag{13}$$

$$A_{2\uparrow}(\mathbf{r}_1,\mathbf{r}') = -\mathcal{D}_\uparrow^{-1}\left\{F_E^{\dagger(0)}(\mathbf{r}_1,\mathbf{r}')\left[\frac{mk_F\cot\alpha_\uparrow}{2\pi\hbar^2} - G_{ER}^{(0)}(\mathbf{r}_1,\mathbf{r}_1)\right] + F_E^{\dagger(0)}(\mathbf{r}_1,\mathbf{r}_1)G_E^{(0)}(\mathbf{r}_1,\mathbf{r}')\right\}, \tag{14}$$

$$\mathcal{D}_\uparrow = \left[\frac{mk_F\cot\alpha_\uparrow}{2\pi\hbar^2} - G_{ER}^{(0)}(\mathbf{r}_1,\mathbf{r}_1)\right]\left[\frac{mk_F\cot\alpha_\downarrow}{2\pi\hbar^2} - G_{-ER}^{(0)*}(\mathbf{r}_1,\mathbf{r}_1)\right] + F_E^{\dagger(0)}(\mathbf{r}_1,\mathbf{r}_1)F_{-E}^{\dagger(0)*}(\mathbf{r}_1,\mathbf{r}_1). \tag{15}$$

To determine $G_{E\downarrow\downarrow}$ and $F^{\dagger}_{E\downarrow\downarrow}$ one should simply swap $\alpha_\uparrow$ and $\alpha_\downarrow$ in Eqs. (11)–(15). The functions $F_{E\alpha\alpha}$ and $\bar{G}_{E\alpha\alpha}$ can be calculated in a similar manner, but we will not write down the corresponding relations here, since the functions $G_{E\alpha\alpha}$ are sufficient to determine all one-particle characteristics.

At this point, it can be seen that the impurity may cause the appearance of additional poles of the Green function at energies when the denominator $\mathcal{D}_\uparrow$ vanishes. As we know, the poles of the Green function at real and almost real energies define the localized states of the system, and thus the zeros of $\mathcal{D}_\uparrow(E)$ must be related to impurity-induced bound or quasibound states.

To complete the calculation of the Green functions, the matrix $\hat{G}_E^{(0)}(\mathbf{r},\mathbf{r}')$ should be determined. This can be done using quasiclassical methods, which are applicable as long as the superconducting coherence length $\xi = \hbar v_F/(\pi|\Delta|)$ is much larger than the Fermi wavelength $\lambda_F = 2\pi k_F^{-1}$ (here, $v_F = \hbar k_F/m$ is the Fermi velocity). A summary of the relevant quasiclassical methods is given in Appendix C. Here, we write down the most important formula for the Green function with close arguments—$|\mathbf{r}-\mathbf{r}'| \ll \xi$:

$$\hat{G}_E^{(0)}(\mathbf{r},\mathbf{r}') = \frac{imk_F}{2\pi\hbar^2}\int \hat{g}_E(\mathbf{r}',\mathbf{n})e^{ik_F\mathbf{n}(\mathbf{r}-\mathbf{r}')}\frac{d^2\mathbf{n}}{4\pi} + \frac{m}{2\pi\hbar^2}\frac{\cos(k_F|\mathbf{r}-\mathbf{r}'|)}{|\mathbf{r}-\mathbf{r}'|}\hat{\tau}_0, \tag{16}$$

where integration goes over a unit sphere, and

$$\hat{g}_E(\mathbf{r},\mathbf{n}) = \begin{pmatrix} g_E(\mathbf{r},\mathbf{n}) & f_E(\mathbf{r},\mathbf{n}) \\ -f_E^{\dagger}(\mathbf{r},\mathbf{n}) & -g_E(\mathbf{r},\mathbf{n}) \end{pmatrix} \tag{17}$$

is the conventional quasiclassical Green function, satisfying the Eilenberger equations [27,28].

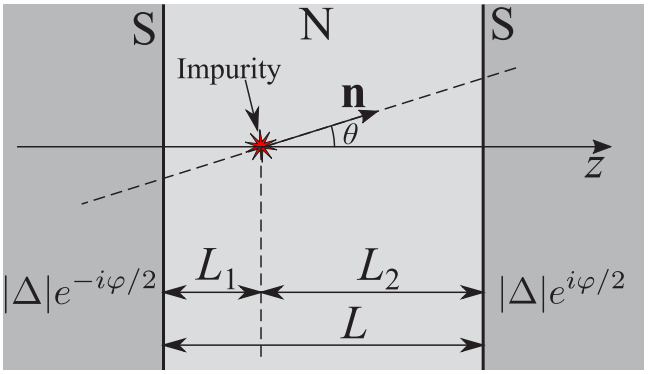

FIG. 2. Infinite SNS junction with a pointlike impurity.

III. SHORT SNS JUNCTION WITH ONE IMPURITY

A. Green functions

Let us apply the theory developed in Sec. II to a short Josephson SNS junction shown in Fig. 2. Let the order parameters in the left and right superconducting banks be equal to $|\Delta|e^{-i\varphi/2}$ and $|\Delta|e^{i\varphi/2}$, respectively. We use a model with an abrupt order parameter profile, which is justified if the characteristic scale of spatial variations of the gap is much smaller than the coherence length, like in superconductor-constriction-superconductor weak links [29]. However, for a start we consider an infinite system and finite-size effects will be discussed in Sec. III D.

We assume that the system contains a point defect located at $\mathbf{r} = \mathbf{r}_1$ in the N layer at distances of L_1 and L_2 from the left and right superconducting banks, respectively. Correspondingly, the total width of the N layer is $L = L_1 + L_2$ and $L \ll \xi$.

To calculate the density of states in the presence of the impurity, we need the Green functions of the pure system. These are determined in Appendix C:

$$G^{(0)}_{ER}(\mathbf{r}_1,\mathbf{r}_1) \approx \frac{mk_F}{4\pi\hbar^2}\left[\cot\left(\gamma(E)+\frac{\varphi}{2}\right)+\cot\left(\gamma(E)-\frac{\varphi}{2}\right)\right], \tag{18}$$

$$F^{\dagger(0)}_{E}(\mathbf{r}_1,\mathbf{r}_1) \approx \frac{mk_F}{4\pi\hbar^2}\left[\sin^{-1}\left(\gamma(E)+\frac{\varphi}{2}\right)+\sin^{-1}\left(\gamma(E)-\frac{\varphi}{2}\right)\right], \tag{19}$$

where

$$\gamma(E) = \arccos\left(\frac{E}{|\Delta|}\right). \tag{20}$$

Corrections to Eqs. (18) and (19) are much smaller than $mk_F/(4\pi\hbar^2)$ as long as

$$|\sin(\gamma(E) \pm \varphi/2)| \sim 1. \tag{21}$$

In particular, estimates of the imaginary parts of the Green functions are given in Appendix D.

B. Quasilocalized states at a nonmagnetic impurity

Now we will focus on the denominator $\mathcal{D}_\uparrow$ of the Green function to find possible localized impurity states. First, we consider a nonmagnetic impurity, such that $\alpha_\uparrow = \alpha_\downarrow = \alpha$. By substituting Eqs. (18) and (19) into Eq. (15) we obtain

$$\mathcal{D}_\uparrow \approx \frac{m^2k_F^2}{4\pi^2\hbar^4}\left[\cot^2\alpha + \frac{\sin^2\gamma(E)}{\sin^2\gamma(E) - \sin^2\frac{\varphi}{2}}\right]. \tag{22}$$

The equation $\mathcal{D}_\uparrow = 0$ can now be solved with respect to $\sin\gamma(E)$: $\sin^2\gamma(E) \equiv 1 - E^2/|\Delta|^2 = \sin^2(\varphi/2)\cos^2\alpha$. Thus the Green functions have a pole at an energy approximately equal to

$$E \approx E_A(\varphi) = |\Delta|\sqrt{1 - \sin^2\frac{\varphi}{2}\cos^2\alpha}. \tag{23}$$

This corresponds to a spin-degenerate Andreev state localized at the impurity. In fact, as stated above, it is a quasibound (resonant) state, since any quasiparticle in the SNS junction can "leak" to infinity along the N layer. Hence the energy of the resonance must have an imaginary part, $E = E_A - iE'_A$, $E'_A > 0$ (the retarded Green function has poles only in the lower complex half-plane). Formally, this happens due to the functions $G^{(0)}_{ER}(\mathbf{r}_1,\mathbf{r}_1)$ and $F^{\dagger(0)}_{E}(\mathbf{r}_1,\mathbf{r}_1)$ having imaginary parts. These imaginary parts and the width of the impurity resonance are estimated in Appendix D. The result for E'_A is

$$E'_A \sim \frac{L}{\xi}|\Delta|\sin^2\frac{\varphi}{2}\sin^4\alpha. \tag{24}$$

Thus, for short Josephson junctions $E'_A \ll \Delta$, so that there is a well-defined resonance. For longer junctions with $L \gtrsim \xi$ there is no resonance.

For completeness, we will describe the structure of the quasibound state. The electronlike part $u(\mathbf{r})$ and a holelike part $v(\mathbf{r})$ of its wave function satisfy the Bogoliubov–de Gennes equations [27]. In a nonmagnetic system these equations are identical to those for the functions $G_{E\alpha\alpha}(\mathbf{r},\mathbf{r}')$ and $F^{\dagger}_{E\alpha\alpha}(\mathbf{r},\mathbf{r}')$ with the only difference being the absence of $\delta(\mathbf{r}-\mathbf{r}')$ in the right-hand side. Hence $u(\mathbf{r})$ and $v(\mathbf{r})$ have the form

$$u(\mathbf{r}) = A_1 G^{(0)}_{E_A}(\mathbf{r},\mathbf{r}_1) + A_2 F^{(0)}_{E_A}(\mathbf{r},\mathbf{r}_1), \tag{25}$$

$$v(\mathbf{r}) = A_1 F^{\dagger(0)}_{E_A}(\mathbf{r},\mathbf{r}_1) - A_2 \bar{G}^{(0)}_{E_A}(\mathbf{r},\mathbf{r}_1), \tag{26}$$

where A_1 and A_2 are some constants. The local density of states at the energy E_A—$\nu(E_A,\mathbf{r})$—is proportional to $|u(\mathbf{r})|^2$. Then, according to Eqs. (C15) and (C16), for $|\mathbf{r}-\mathbf{r}_1| \gg \lambda_F$ the envelope of the density of states decays as

$$\nu(E_A,\mathbf{r}) \propto |\mathbf{r}-\mathbf{r}_1|^{-2}\exp\left(-\frac{2\sqrt{|\Delta|^2 - E_A^2}}{\hbar v_F}|\mathbf{r}-\mathbf{r}_1|\right). \tag{27}$$

Additionally, $\nu(E_A,\mathbf{r})$ exhibits spatial oscillations with the period $\lambda_F/2$. In this respect, the impurity-induced quasibound state resembles the Shiba state induced by a magnetic impurity in a bulk superconductor [6–8]. The main difference from the Shiba state is the strong anisotropy of the $\nu(E_A,\mathbf{r})$ profile, as can be seen in Fig. 3.

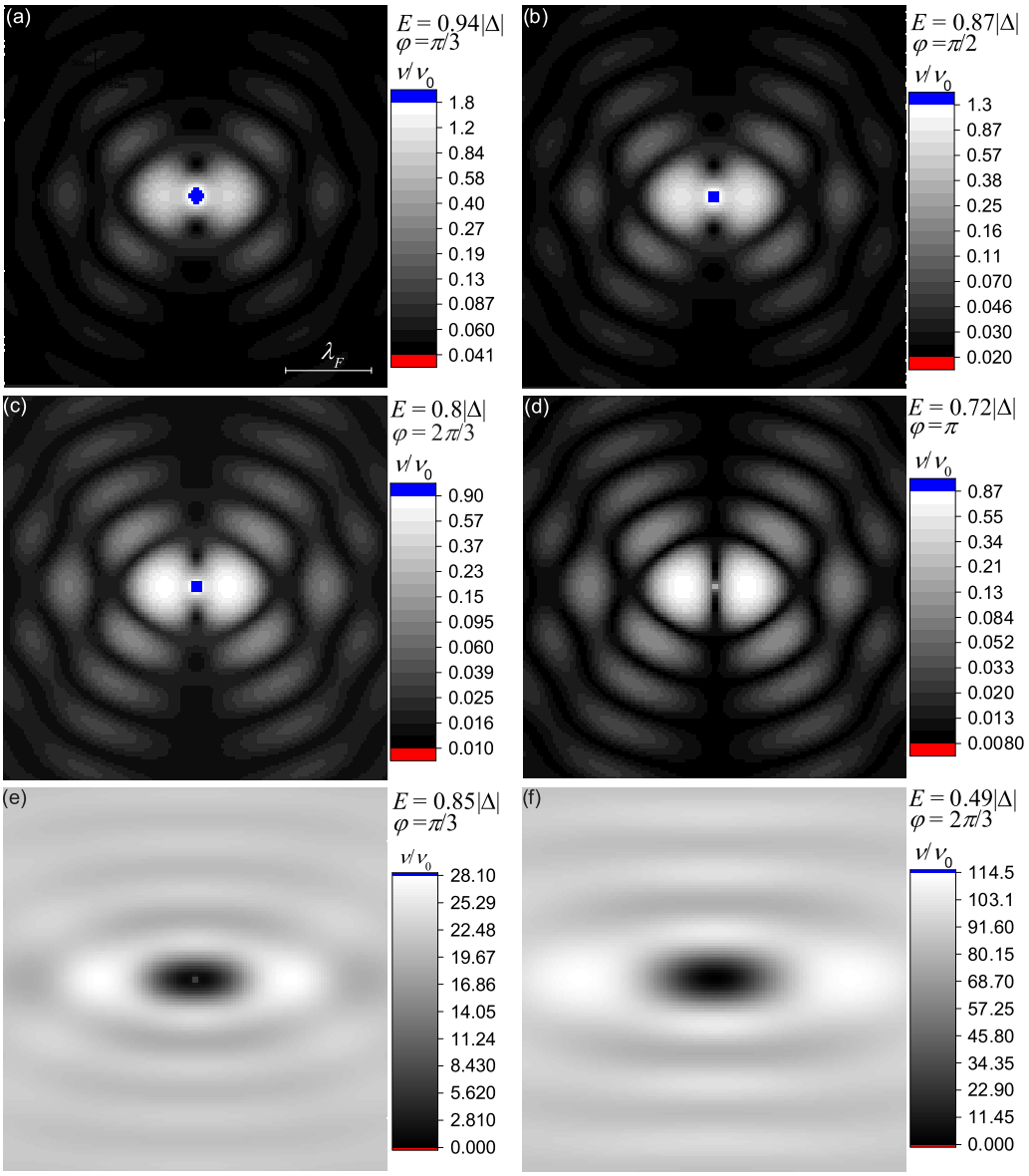

FIG. 3. Spatial profiles of the density of states [Eq. (6)] in a plane passing through the z axis and through the impurity—see Fig. 2. $\nu(E,\mathbf{r})$ is measured in units of the density of states in a normal metal—$\nu_0 = m/(\hbar^2\lambda_F)$. In all graphs, $\alpha = 0.81$, $L/\xi = 1/20$, the impurity is located in the center of the N layer (and in the center of the pictures), and the size of the area shown is $4.46\lambda_F \times 4.46\lambda_F$. The coherence length is assumed much larger than the dimensions of this area, so for the Green function of a clean system Eqs. (16), (C9), and (C10) are used (with the integral evaluated numerically). (a)–(d) Profiles of the impurity state for different values of φ: $E = E_A(\varphi)$. Note the logarithmic color scale, which is used to make several oscillations of $\nu(E_A,\mathbf{r})$ visible. (e), (f) Profiles of $\nu(E,\mathbf{r})$ at energies close to the peak of the density of states of a clean junction: $E \approx |\Delta|\cos(\varphi/2)$.

C. Quasilocalized states at a magnetic impurity

Here we will generalize the results of the previous section for the case of a magnetic impurity, when $\alpha_\uparrow \neq \alpha_\downarrow$. Using Eqs. (15), (18), and (19), we can write the determinant $\mathcal{D}_\uparrow$ in the following form:

$$\mathcal{D}_\uparrow \approx \frac{m^2k_F^2[\cos(2\Theta) - \cos(2\gamma - \alpha_\uparrow + \alpha_\downarrow)]}{4\pi^2\hbar^4 \sin\alpha_\uparrow \sin\alpha_\downarrow [\cos\varphi - \cos(2\gamma)]}, \tag{28}$$

where

$$\Theta = \arcsin\sqrt{\cos\alpha_\uparrow \cos\alpha_\downarrow \sin^2\frac{\varphi}{2} + \sin^2\left(\frac{\alpha_\uparrow - \alpha_\downarrow}{2}\right)}. \tag{29}$$

Equating $\mathcal{D}_\uparrow$ to zero, we obtain

$$\sin\left(\gamma + \frac{\alpha_\downarrow - \alpha_\uparrow}{2} - \Theta\right)\sin\left(\gamma + \frac{\alpha_\downarrow - \alpha_\uparrow}{2} + \Theta\right) = 0$$

or

$$\gamma = \frac{\alpha_\uparrow - \alpha_\downarrow}{2} \pm \Theta + \pi n, \tag{30}$$

where n is an integer. To determine the valid values of n we take into account that $\gamma \in [0,\pi]$. As follows from Eq. (29),

$$\left|\frac{\alpha_\uparrow - \alpha_\downarrow}{2}\right| < \Theta < \frac{\pi}{2}.$$

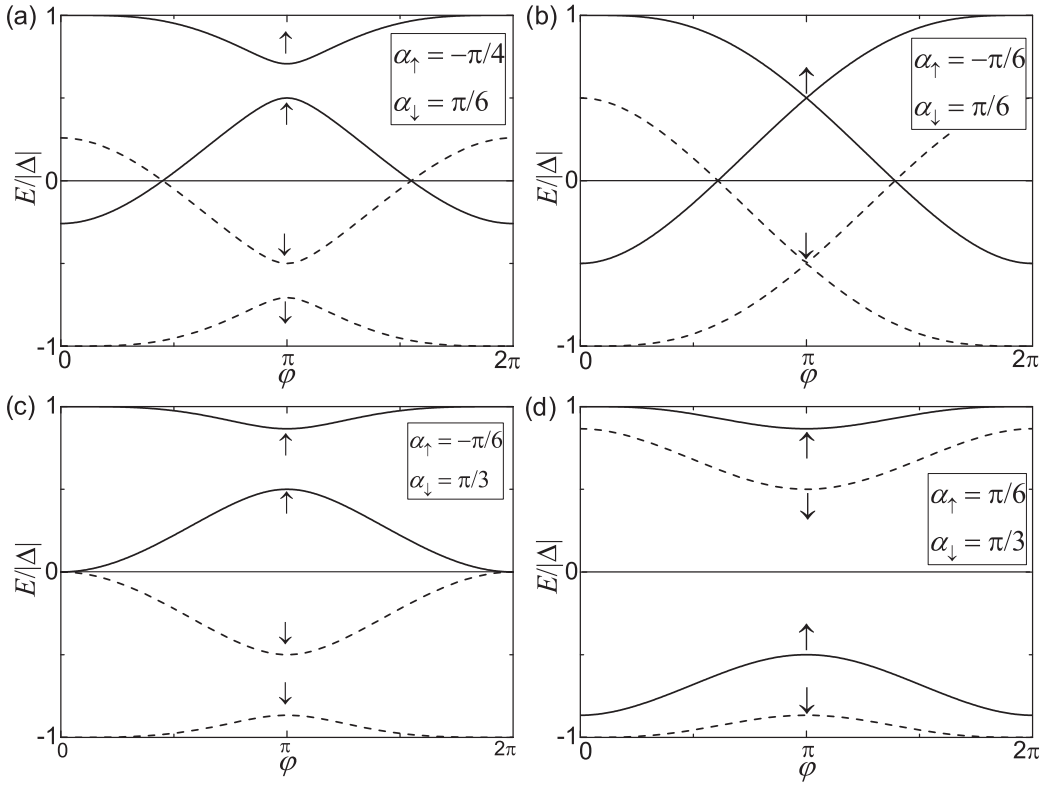

FIG. 4. Energies of "spin-up" (↑) and "spin-down" (↓) impurity states in a short SNS junction. In (b) a special case is depicted, when $\alpha_\uparrow + \alpha_\downarrow = 0$, and there is no gap between the branches of $E(\varphi)$ with the same spin.

Hence γ can only take the values

$$\gamma = \frac{\alpha_\uparrow - \alpha_\downarrow}{2} + \frac{\pi}{2} \pm \left(\frac{\pi}{2} - \Theta\right). \tag{31}$$

This yields the real parts of the energies of quasibound "spin-up" impurity states:

$$E_\uparrow = |\Delta| \sin\left(\frac{\alpha_\downarrow - \alpha_\uparrow}{2} \pm \left(\frac{\pi}{2} - \Theta\right)\right). \tag{32}$$

For "spin-down" quasiparticles, we need to swap $\alpha_\uparrow$ and $\alpha_\downarrow$:

$$E_\downarrow = |\Delta| \sin\left(\frac{\alpha_\uparrow - \alpha_\downarrow}{2} \pm \left(\frac{\pi}{2} - \Theta\right)\right). \tag{33}$$

Similar relations have been previously derived for Andreev states in a short Josephson junction with a ferromagnetic barrier [30]. As before, the energies of the impurity states have imaginary parts of the order of $|\Delta|L/\xi$.

Equations (32) and (33) give four values of the energy, two of them being positive and two being negative, except for the case when some values are exactly zero. Of course, the Bogoliubov quasiparticles have positive energies; thus there are generally two quasibound states localized by a magnetic impurity.

Let us consider some particular cases. When $\alpha_\uparrow = \alpha_\downarrow = \alpha$ we have $E_\uparrow = \pm E_A$ and $E_\downarrow = \pm E_A$ [Eq. (23)], in accordance with Sec. III B. When $\varphi = 0$, we should obtain the energies of Shiba states in a bulk superconductor. Indeed, one can see that in this case the positive values of $E_\uparrow$ and $E_\downarrow$ are $|\Delta|$ and $|\Delta||\cos(\alpha_\uparrow - \alpha_\downarrow)|$, the latter being the energy of the Shiba state with zero orbital momentum [8].

For a nonmagnetic impurity the dependence of E_A on φ is qualitatively similar for all values of the phase α, and has no zero crossings: $E_A \geqslant 0$. For a magnetic impurity qualitatively different behaviors of the bound state energies vs φ are possible depending on $\alpha_\uparrow$ and $\alpha_\downarrow$. To illustrate this, we first calculate the zero crossings of $E_\uparrow(\varphi)$ and $E_\downarrow(\varphi)$. Using the fact that $\gamma(0) = \pi/2$, we find from Eq. (31) that at least one branch of both $E_\uparrow(\varphi)$ and $E_\downarrow(\varphi)$ takes the value zero when

$$\sin^2\frac{\varphi}{2} = \frac{\cos(\alpha_\uparrow - \alpha_\downarrow)}{\cos\alpha_\uparrow \cos\alpha_\downarrow}. \tag{34}$$

Hence zero crossings are present if and only if the following conditions are met:

$$\cos(\alpha_\uparrow - \alpha_\downarrow) > 0, \tag{35}$$

$$\sin\alpha_\uparrow \sin\alpha_\downarrow < 0. \tag{36}$$

At each crossing point one branch of $E_\uparrow(\varphi)$ goes from positive to negative with growing φ, and one branch of $E_\downarrow(\varphi)$ goes from negative to positive, or vice versa. Such a situation is depicted in Figs. 4(a) and 4(b).

Consider the case when one of the conditions (35) or (36) is violated—both conditions can be violated only in the degenerate case when one of the scattering phases equals $\pm\pi/2$, so that $E_\uparrow$ and $E_\downarrow$ do not depend on φ. If $\cos(\alpha_\uparrow - \alpha_\downarrow) \leqslant 0$, for all values of φ there are two bound states with the same spin. In particular, there are two "spin-up" states for

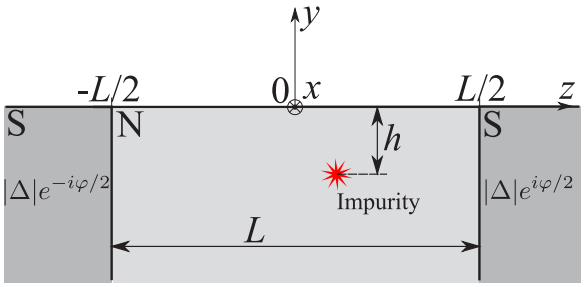

FIG. 5. Semi-infinite SNS junction with an impurity.

$\alpha_\downarrow > \alpha_\uparrow$ ($E_\uparrow \geqslant 0$) and two "spin-down" states for $\alpha_\downarrow < \alpha_\uparrow$ ($E_\downarrow \geqslant 0$)—see Fig. 4(c). On the contrary, when the condition (36) is violated, we have one spin-up and one spin-down state for all φ—see Fig. 4(d).

D. Semi-infinite SNS junction

In the previous sections we studied the impurity states in an idealized spatially unlimited system, so the obtained results cannot be directly applied to real structures, which have boundaries. In this section, we will analyze how the impurity states are affected by a flat surface. In particular, we consider here a SNS junction occupying the half-space $y < 0$—see Fig. 5. The half-space $y > 0$ is occupied by vacuum or an insulator. An impurity is located at the point $\mathbf{r}_1 = (x_1, -h, z_1)$ inside the normal layer.

We assume that there is an infinitely high potential barrier at the surface of the junction, so that the following boundary condition should be imposed:

$$\check{G}(\mathbf{r},\mathbf{r}')|_{y=0} = 0. \tag{37}$$

Then, the Green function without the impurity, which we will denote as $\hat{G}_E^{(S)}(\mathbf{r},\mathbf{r}')$, can be determined using the image method:

$$\hat{G}_E^{(S)}(\mathbf{r},\mathbf{r}') = \hat{G}_E^{(0)}(\mathbf{r},\mathbf{r}') - \hat{G}_E^{(0)}(\mathbf{r},\mathbf{r}''), \tag{38}$$

where by $\hat{G}_E^{(0)}(\mathbf{r},\mathbf{r}')$ we mean the Green function of a pure infinite junction, $\mathbf{r}' = (x',y',z')$, and $\mathbf{r}'' = (x', -y', z')$. Let us assume that h is much smaller than the coherence length ξ. Using Eqs. (C17) and (C27), we find that the regular part of the Green function is

$$\begin{aligned} G_{ER}^{(S)}(\mathbf{r}_1,\mathbf{r}_1) &\equiv G_{ER}^{(0)}(\mathbf{r}_1,\mathbf{r}_1) - G_E^{(0)}(\mathbf{r}_1,\mathbf{r}_1 + 2h\mathbf{y}_0) \\ &= G_{ER}^{(0)}(\mathbf{r}_1,\mathbf{r}_1)\left[1 - \frac{\sin(2k_F r)}{2k_F r}\right] \\ &\quad - \frac{m\cos(2k_F h)}{4\pi\hbar^2 h}, \end{aligned} \tag{39}$$

where $\mathbf{y}_0$ is a unit vector directed along the y axis and $G_{ER}^{(0)}(\mathbf{r}_1,\mathbf{r}_1)$ is given by Eq. (18). Similarly,

$$F_E^{\dagger(S)}(\mathbf{r}_1,\mathbf{r}_1) = F_E^{\dagger(0)}(\mathbf{r}_1,\mathbf{r}_1)\left[1 - \frac{\sin(2k_F r)}{2k_F r}\right], \tag{40}$$

with $F_E^{\dagger(0)}(\mathbf{r}_1,\mathbf{r}_1)$ given by Eq. (19). If we substitute $G_{ER}^{(S)}(\mathbf{r}_1,\mathbf{r}_1)$ and $F_E^{\dagger(S)}(\mathbf{r}_1,\mathbf{r}_1)$ into Eq. (15), after some algebra we may find

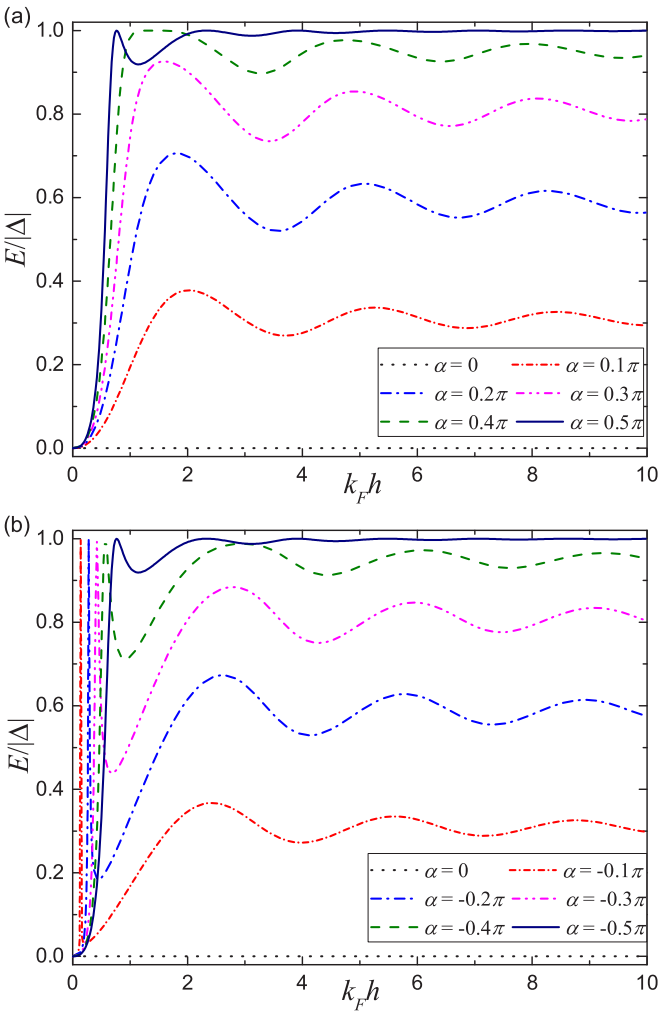

FIG. 6. Dependencies of the impurity state energy E on the distance h between the impurity and the surface of the SNS junction for $\varphi = \pi$. The scattering phases α are positive in graph (a) and negative in graph (b).

that the equations for the impurity states take the same form as for an infinite junction with the scattering phases replaced by effective values $\alpha_{\mathrm{eff}\uparrow,\downarrow}$, which are defined as follows:

$$\cot\alpha_{\mathrm{eff}\uparrow,\downarrow} = \frac{\cot\alpha_{\uparrow,\downarrow} + \frac{\cos(2k_F h)}{2k_F h}}{1 - \frac{\sin(2k_F h)}{2k_F h}}. \tag{41}$$

Note that $h = 0$ results in $\alpha_{\mathrm{eff}\uparrow,\downarrow} = 0$, i.e., there is effectively no impurity. A remarkable feature of Eq. (41) is the oscillating $\alpha_{\mathrm{eff}\uparrow,\downarrow}$ vs h dependence, which results in the energies of the impurity states also oscillating when h is changed. This simple example illustrates the mesoscopic fluctuations in a system with one impurity. These fluctuations decay on a length scale of the order of k_F^{-1}, and hence the influence of the surface on the energies of the impurity states is small when h is much larger than the Fermi wavelength.

Typical energy vs h graphs for a nonmagnetic impurity are shown in Fig. 6.

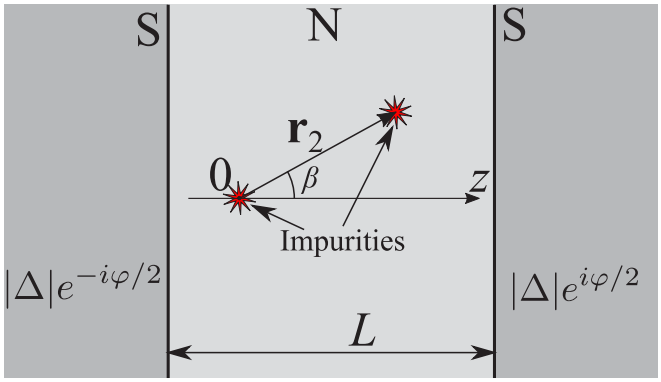

FIG. 7. SNS junction with two impurities.

IV. BOUND STATES IN A SHORT SNS JUNCTION WITH TWO IMPURITIES

In this section we will determine the energies of resonant states in a short SNS junction with two impurities. The system under consideration is shown in Fig. 7. Here, one impurity with a scattering phase α_1 is located at the origin. The other impurity with a scattering phase α_2 is located at the point $\mathbf{r}_2 = (x_2, y_2, z_2)$, such that $z_2 \geqslant 0$. The vector $\mathbf{r}_2$ makes an angle β with the z axis.

As before, we can find the impurity states in this system by calculating the poles of the Green function. However, even with only two impurities this method becomes very laborious. For this reason, we will use here a different method developed by Beenakker [31], which yields the energies of all Andreev states in short nonmagnetic Josephson junctions ($L \ll \xi$). These energies have the form

$$E_i(\varphi) = |\Delta|\sqrt{1 - T_i \sin^2 \frac{\varphi}{2}}, \tag{42}$$

where T_i is an eigenvalue of the matrix $\hat{T} = \hat{t}\hat{t}^\dagger$, with $\hat{t}$ being the transmission matrix of electrons with the energy μ ($E = 0$) through the normal layer. For the Andreev states that are not affected by impurities one has ideal transmission, i.e., $T_i = 1$. Hence the impurity-induced states correspond to nonunit values of T_i. Note that Eq. (23) is a particular case of Eq. (42) with $T_i = \cos^2 \alpha$. Thus the central result of Sec. III B can be also interpreted as follows: a single nonmagnetic impurity with a scattering phase α affects one transport channel in the normal layer, reducing the transparency of this channel from unity to $\cos^2 \alpha$.

The coefficients T_i for the case of two point impurities are calculated in Appendix E. It is shown that all coefficients T_i are equal to unity except for two, which we denote as T_1 and T_2. Hence we have two quasibound states per spin projection.

The general expressions for T_1 and T_2 are rather cumbersome [Eqs. (E16), (E17), and (E19)], but we can analyze some limiting cases. For example, if the impurities are very close to each other—$k_F r_2 \ll 1$—they are equivalent to one impurity with a scattering phase α_0 given by Eq. (E22).

When the distance between the impurities is larger—$k_F r_2 \gtrsim 1$—the coefficients T_1 and T_2 are oscillating functions of both β and r_2, as can be seen in Fig. 8. Thus we have another example of sample-to-sample fluctuations of the impurity state energies, somewhat similar to those present in a semi-infinite junction (Sec. III D).

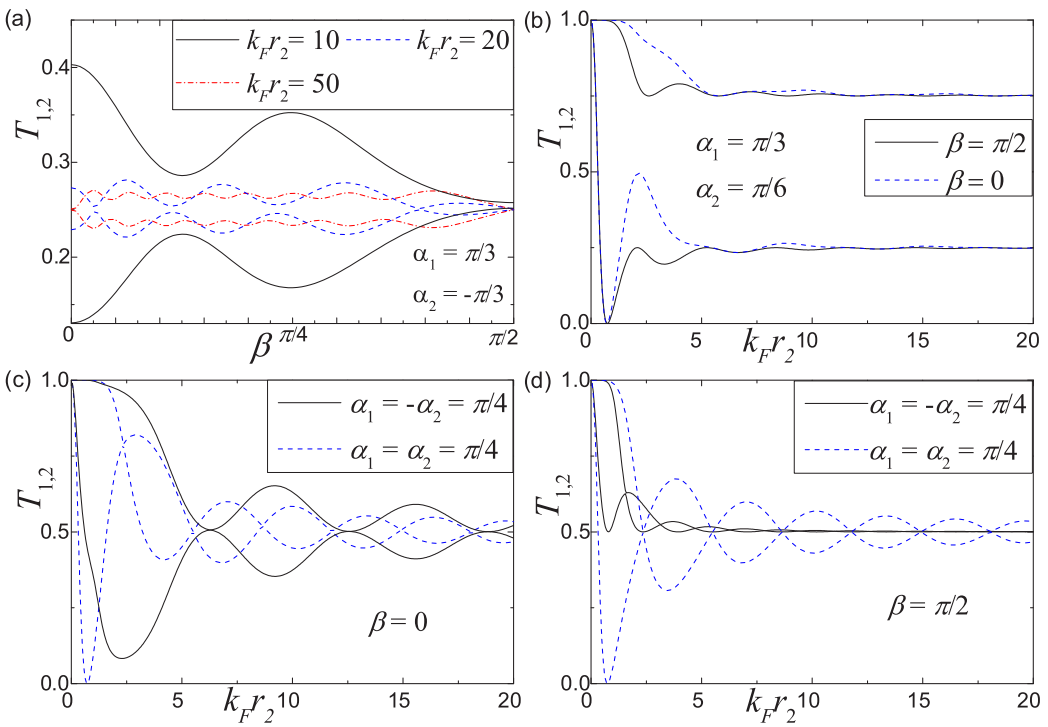

FIG. 8. (a) Dependencies of $T_{1,2}$ [Eq. (E19)] on β for several values of r_2. (b)–(d) Dependencies of $T_{1,2}$ on r_2 for various values of α_1, α_2, and β. It can be seen that with growing r_2 the transparencies $T_{1,2}$ approach their asymptotic values significantly faster when $|\alpha_1| \neq |\alpha_2|$ than in the case when $|\alpha_1| = |\alpha_2|$.

At $k_F r_2 \ll 1$ one expects that the impurities are more or less independent, so that $T_{1,2} \approx \cos^2 \alpha_{1,2}$. One can prove (see Appendix E) that the differences between T_1, T_2 and their asymptotic values are of the order of $(k_F r_2)^{-2}$ when $|\alpha_1| \neq |\alpha_2|$ and of the order of $(k_F r_2)^{-1}$ when $|\alpha_1| = |\alpha_2|$.

V. OBSERVABLE IMPLICATIONS

Let us discuss observable implications of the results above. First, individual impurity states can be observed using the STM technique [32], which has been recently applied for the visualization of Shiba states in a 2D superconductor [33]. This technique allows one to determine the energies of the resonant states as well as their approximate spatial structure.

Second, the impurities certainly affect the transport characteristics of the Josephson junction. Using the theory of Beenakker [31] for short SNS junctions, we can estimate the influence of defects on the Josephson current. This current is given by

$$I(\varphi) = \frac{e|\Delta|^2}{2\hbar} \sin\varphi \sum_i \frac{T_i}{E_i(\varphi)} \tanh\left(\frac{E_i(\varphi)}{2T}\right), \tag{43}$$

where e is the elementary charge, $E_i(\varphi)$ is given by Eq. (42), T is the temperature, and summation goes over all eigenvalues T_i of the matrix $\hat{t}\hat{t}^\dagger$. Without impurities, the current is

$$I_0(\varphi) = \frac{e|\Delta|N}{\hbar} \sin(\varphi/2) \tanh\left(\frac{|\Delta|\cos(\varphi/2)}{2T}\right), \tag{44}$$

If we add one impurity, it switches one transmission eigenvalue from $T_i = 1$ to $T_i = \cos^2\alpha$, and the current is modified by a value

$$\delta I(\varphi) = \frac{e|\Delta|}{2\hbar} \sin\varphi \left[\cos^2\alpha \frac{\tanh\left(\frac{|\Delta|\sqrt{1-\cos^2\alpha\,\sin^2(\varphi/2)}}{2T}\right)}{\sqrt{1-\cos^2\alpha\,\sin^2(\varphi/2)}} - \frac{1}{\cos(\varphi/2)} \tanh\left(\frac{|\Delta|\cos(\varphi/2)}{2T}\right)\right]. \tag{45}$$

As we have seen, two identical impurities separated by a distance much larger than k_F^{-1} switch two eigenvalues T_i to $\cos^2\alpha$. This fact can be generalized: a sufficiently small amount of evenly distributed impurities n in a junction with many channels—$N \gg 1$—should change n eigenvalues T_i from unity to $\cos^2\alpha$. Here, "suffiently small amount" means at least $n \ll N$; however, the actual restriction might be stronger and its derivation is beyond the scope of this work. If the defects are distributed randomly in the N layer, of course, there is a chance that the distance between some defects is $\lesssim k_F^{-1}$, and also some defects may be located near the boundary of the junction. However, on the average the number of such impurities is much smaller than n, provided that $N \gg 1$ and $n \ll N$. Thus we may conclude that the average contribution of n point impurities to the Josephson current is $n\delta I(\varphi)$. Then, the averaged over many samples Josephson current is

$$\bar{I}(\varphi) = I_0(\varphi) + \bar{n}\delta I(\varphi), \tag{46}$$

where $\bar{n}$ denotes the average number of defects in the N layer. If the quantity n obeys a Poisson distribution, the root-mean-square deviation of the current from its average is

$$\sqrt{\overline{(I-\bar{I})^2}} = \bar{n}|\delta I(\varphi)|. \tag{47}$$

In a similar way, we can calculate the normal-state conductance G of the N layer. In the presence of n impurities, according to Landauer's formula [34], the conductance is given by

$$G = \frac{2e^2}{\pi\hbar}(N - n\,\sin^2\alpha). \tag{48}$$

This can be interpreted as each impurity effectively reducing the cross section of the N layer by the scattering cross section σ_S [Eq. (B6)]. Now we can also determine the average conductance and its root-mean-square deviation from the average:

$$\bar{G} = \frac{2e^2}{\pi\hbar}(N - \bar{n}\,\sin^2\alpha), \tag{49}$$

$$\sqrt{\overline{(G-\bar{G})^2}} = \frac{2e^2}{\pi\hbar}\bar{n}\,\sin^2\alpha. \tag{50}$$

Equations (47) and (50) give the Josephson current and conductance fluctuations in the low-disorder limit, complementing Beenakker's results [31] derived in the limit of a diffusive N layer.

VI. CONCLUSION

In conclusion, we have analyzed the subgap spectral features due to nonmagnetic and magnetic point impurities in a short clean SNS junction. A single defect induces two quasibound states, which are somewhat similar to Shiba states in a uniform superconductor. The energies of the impurity states are given by Eqs. (32) and (33) [which simplify to Eq. (23) in the case of a nonmagnetic defect], and the widths of the resonances are of the order of $|\Delta|L/\xi$. If the defect is close to a flat surface of the junction, the impurity state energies exhibit decaying oscillations as a function of the distance h between the impurity and the sample surface.

We have also studied a system with two nonmagnetic impurities, as shown on Fig. 7. Here, there are two quasilocalized states per spin projection, the energies of which depend in a complex manner on both the length and orientation of the vector $\mathbf{r}_2$ connecting the impurities.

Finally, we have derived the sample-to-sample fluctuations of the Josephson current and normal-state conductance of the junction in the pure limit, i.e., in the presence of a relatively small amount of impurities.

ACKNOWLEDGMENTS

I am very grateful to A. S. Mel'nikov for stimulating discussions and for thorough reading of this paper. The work has been supported by Russian Science Foundation Grant No. 17-12-01383 (Secs. II and III), Foundation for the advancement of theoretical physics BASIS Grant No. 109 (Sec. IV), and Russian Foundation for Basic Research Grant No. 18-02-00390 (Sec. V).

APPENDIX A: DEFINITIONS OF THE GREEN FUNCTIONS

In this paper we use the following definition of the real-time retarded Green functions:

$$G_{\alpha\beta}(\mathbf{r},\mathbf{r}',t) = i\langle\psi_\alpha(\mathbf{r},t)\psi^\dagger_\beta(\mathbf{r}') + \psi^\dagger_\beta(\mathbf{r}')\psi_\alpha(\mathbf{r},t)\rangle_T, \quad \text{(A1)}$$

$$F^\dagger_{\alpha\beta}(\mathbf{r},\mathbf{r}',t) = \sum_\gamma \sigma_{y\alpha\gamma}\langle\psi^\dagger_\gamma(\mathbf{r},t)\psi^\dagger_\beta(\mathbf{r}') + \psi^\dagger_\beta(\mathbf{r}')\psi^\dagger_\gamma(\mathbf{r},t)\rangle_T, \quad \text{(A2)}$$

$$F_{\alpha\beta}(\mathbf{r},\mathbf{r}',t) = \sum_\gamma \sigma_{y\beta\gamma}\langle\psi_\alpha(\mathbf{r},t)\psi_\gamma(\mathbf{r}') + \psi_\gamma(\mathbf{r}')\psi_\alpha(\mathbf{r},t)\rangle_T, \quad \text{(A3)}$$

$$\bar{G}_{\alpha\beta}(\mathbf{r},\mathbf{r}',t) = i\sum_{\gamma\epsilon}\sigma_{y\alpha\gamma}\sigma_{y\beta\epsilon}\langle\psi^\dagger_\gamma(\mathbf{r},t)\psi_\epsilon(\mathbf{r}') + \psi_\epsilon(\mathbf{r}')\psi^\dagger_\gamma(\mathbf{r},t)\rangle_T \quad \text{(A4)}$$

for $t > 0$, and $G_{\alpha\beta} = F^\dagger_{\alpha\beta} = F_{\alpha\beta} = \bar{G}_{\alpha\beta} = 0$ for $t < 0$. Here, $\langle\cdots\rangle_T$ denotes the thermodynamic average and $\psi_\alpha(\mathbf{r},t)$ is the Heisenberg operator:

$$\psi_\alpha(\mathbf{r},t) = \exp(i\mathcal{H}t/\hbar)\psi_\alpha(\mathbf{r})\exp(-i\mathcal{H}t/\hbar). \quad \text{(A5)}$$

The matrices with the subscript "E," appearing in Eq. (5), are the Fourier transforms of the matrices given by Eqs. (A1)–(A4) with respect to t. Note that our definitions of the Green functions are somewhat different from those used by Kopnin [27]. In our case, it is convenient to incorporate the $\hat{\sigma}_y$ matrices in the definitions (A1)–(A4) to eliminate them in the Gor'kov equation (4).

APPENDIX B: GREEN FUNCTION OF A NORMAL SYSTEM WITH A POINT IMPURITY

In this Appendix we illustrate our method of calculating the Green function in the presence of a point defect by a relatively simple example of a normal system. The problem of scattering of a free particle by δ-type potentials has been previously extensively studied in literature. A summary of the main obtained results and their strict derivations can be found in Ref. [35]. Here, in a somewhat voluntary way we extend the previous results to the case of an inhomogeneous 3D system with a defect.

We will determine the retarded Green function $G_E(\mathbf{r},\mathbf{r}')$ of the following Schrödinger equation:

$$[H_0(\mathbf{r}) + U_0(\mathbf{r}) + V(\mathbf{r}-\mathbf{r}_1) - E - i\epsilon^+]G_E(\mathbf{r},\mathbf{r}') = \delta(\mathbf{r}-\mathbf{r}'), \quad \text{(B1)}$$

where $H_0(\mathbf{r})$ is given by Eq. (2), $V(\mathbf{r})$ is the potential of a pointlike impurity, and $U_0(\mathbf{r})$ is some electric potential not related to the impurity. For simplicity, we put the impurity outside the range of the potential $U_0(\mathbf{r})$, so that $U_0(\mathbf{r}_1) = 0$.

We will assume that the solution $G^{(0)}_E(\mathbf{r},\mathbf{r}')$ of Eq. (B1) without the impurity [with $V(\mathbf{r}) = 0$] is known. It has a regular part and a singularity, which we separate explicitly:

$$G^{(0)}_E(\mathbf{r},\mathbf{r}') = \frac{m}{2\pi\hbar^2|\mathbf{r}-\mathbf{r}'|} + G^{(0)}_{ER}(\mathbf{r},\mathbf{r}'), \quad \text{(B2)}$$

where $G^{(0)}_{ER}(\mathbf{r},\mathbf{r}')$ is a regular function at all arguments.

In the presence of the impurity, assuming that it is small enough so that only spherically symmetric scattering can be taken into account, we can write the solution of Eq. (B1) in the form

$$G_E(\mathbf{r},\mathbf{r}') = G_{\text{in}}(\mathbf{r},\mathbf{r}') + C\frac{G_{\text{in}}(\mathbf{r}_1,\mathbf{r}')e^{ik|\mathbf{r}-\mathbf{r}_1|}}{k|\mathbf{r}-\mathbf{r}_1|}, \quad \text{(B3)}$$

where the function $G_{\text{in}}(\mathbf{r},\mathbf{r}')$ is regular at $\mathbf{r} = \mathbf{r}_1$ and represents an incoming wave, k is the wave number of a free electron, and C is a coefficient that depends on the impurity potential. By virtue of Hermiticity of the Hamiltonian, a relation between the imaginary part of C and its modulus exists, namely

$$\text{Im}(C) = |C|^2, \quad \text{(B4)}$$

which is a corollary of the so-called optical theorem. Its derivation can be found in textbooks [35,36]. Equation (B4) implies that C can be written as

$$C = e^{i\alpha}\sin\alpha, \quad \text{(B5)}$$

where α is the energy-dependent scattering phase of the impurity. Note that C is π periodic in α, so we may confine α to the range $[-\pi/2,\pi/2]$, with $\alpha = \pm\pi/2$ corresponding to the so-called unitary limit. The opposite Born approximation limit corresponds to $|\alpha| \ll 1$. The scattering cross section of the impurity is given by

$$\sigma_S = 4\pi k^{-2}\sin^2\alpha. \quad \text{(B6)}$$

For the following it is more convenient to rewrite Eq. (B3) in the form

$$G_E(\mathbf{r},\mathbf{r}') = G_{ER}(\mathbf{r},\mathbf{r}') + \frac{G_{ER}(\mathbf{r}_1,\mathbf{r}')\tan\alpha}{k|\mathbf{r}-\mathbf{r}_1|}, \quad \text{(B7)}$$

where

$$G_{ER}(\mathbf{r},\mathbf{r}') = G_{\text{in}}(\mathbf{r},\mathbf{r}') + G_{\text{in}}(\mathbf{r}_1,\mathbf{r}')e^{i\alpha}\sin\alpha\frac{e^{ik|\mathbf{r}-\mathbf{r}'|}-1}{k|\mathbf{r}-\mathbf{r}'|} \quad \text{(B8)}$$

is another regular function at $\mathbf{r} = \mathbf{r}_1$. Now, one can see that $G_E(\mathbf{r},\mathbf{r}')$ and $G^{(0)}_E(\mathbf{r},\mathbf{r}_1)$ have the same $|\mathbf{r}-\mathbf{r}_1|^{-1}$ singularity, and hence the solution of Eq. (B1) can be also written as

$$G_E(\mathbf{r},\mathbf{r}') = G^{(0)}_E(\mathbf{r},\mathbf{r}') + G^{(0)}_E(\mathbf{r},\mathbf{r}_1)A(\mathbf{r}_1,\mathbf{r}'), \quad \text{(B9)}$$

where $A(\mathbf{r}_1,\mathbf{r}')$ is a function to be determined. Indeed, the function given by Eq. (B9) has the correct asymptotic behavior near the defect [Eq. (B7)], and also satisfies Eq. (B1) when $\mathbf{r}$ and $\mathbf{r}'$ lie outside the range of the impurity potential.

To calculate $A(\mathbf{r}_1,\mathbf{r}')$ we note that Eqs. (B7) and (B9) should give the same function $G_E(\mathbf{r},\mathbf{r}')$. After extracting the regular part of the right-hand side of Eq. (B9) at $\mathbf{r} = \mathbf{r}_1$ by using Eq. (B2) with $\mathbf{r}' = \mathbf{r}_1$, we obtain the algebraic equation

$$\frac{mA(\mathbf{r}_1,\mathbf{r}')}{2\pi\hbar^2} = \frac{\tan\alpha}{k_F}\left[G^{(0)}_E(\mathbf{r}_1,\mathbf{r}') + A(\mathbf{r}_1,\mathbf{r}')G^{(0)}_{ER}(\mathbf{r}_1,\mathbf{r}_1)\right]. \quad \text{(B10)}$$

Here, we replace k with the Fermi wave number k_F, assuming that $|E| \ll \mu$. After solving Eq. (B10), we obtain the Green

function

$$G_E(\mathbf{r},\mathbf{r}') = G_E^{(0)}(\mathbf{r},\mathbf{r}') + \frac{G_E^{(0)}(\mathbf{r},\mathbf{r}_1)G_E^{(0)}(\mathbf{r}_1,\mathbf{r}')}{\frac{mk_F\cot\alpha}{2\pi\hbar^2} - G_{ER}^{(0)}(\mathbf{r}_1,\mathbf{r}_1)}. \quad \text{(B11)}$$

It is important that Eq. (B11) gives the exact Green function when both $\mathbf{r}$ and $\mathbf{r}'$ lie outside the impurity. If desired, Born approximations of any order can be deduced from Eq. (B11). Thus our result should be identical to the result obtained using the T-matrix method, which involves the summation of diagrams corresponding to Born approximations of all orders. Indeed, the reader may check that the T-matrix method yields Eq. (B11) in the spatially homogeneous case [when $U_0(\mathbf{r}) = 0$] [3].

Finally, we shortly discuss how to generalize the obtained result for a magnetic impurity. The Green function $\hat{G}_E$ and the impurity potential $\hat{V}(\mathbf{r})$ then will be 2×2 matrices in spin space. One typically writes the potential in the form (3). If we direct the spin quantization axis along the impurity spin [parallel to $\mathbf{J}(\mathbf{r})$], electrons with spin "up" and spin "down" will have different scattering phases—$\alpha_\uparrow$ and $\alpha_\downarrow$, respectively. Then, the components of the matrix Green function $\hat{G}_E$ with spin indices $\uparrow\downarrow$ and $\downarrow\uparrow$ vanish, and the components with indices $\uparrow\uparrow$ or $\downarrow\downarrow$ are still given by Eq. (B11), where α is replaced with $\alpha_\uparrow$ or $\alpha_\downarrow$, respectively.

APPENDIX C: QUASICLASSICAL CALCULATION OF THE GREEN FUNCTIONS IN CLEAN SUPERCONDUCTORS

In this Appendix we will recall some old results concerning the quasiclassical methods applied to clean superconductors, and we will derive Eq. (16). In the end, expressions for the Green functions with noncoinciding arguments for a short SNS junction will be given.

Gor'kov and Kopnin [37] pointed out that in a clean system without potential barriers it is convenient to write the Green function $\hat{G}_E^{(0)}(\mathbf{r},\mathbf{r}')$ at $k_F|\mathbf{r}-\mathbf{r}'|\gg 1$ in the following form:

$$\hat{G}_E^{(0)}(\mathbf{r},\mathbf{r}') = \frac{m}{2\pi\hbar^2 R}[\hat{g}_{E+}(\mathbf{r}',R,\mathbf{n})e^{ik_F R} + \hat{g}_{E-}(\mathbf{r}',R,\mathbf{n})e^{-ik_F R}], \quad \text{(C1)}$$

where $R = |\mathbf{r}-\mathbf{r}'|$ and $\mathbf{n} = (\mathbf{r}-\mathbf{r}')/R$ is a unit vector. In the limit $\xi \gg k_F^{-1}$ a set of quasiclassical equations for $\hat{g}_E^+$ and $\hat{g}_E^-$ can be derived. By substituting Eq. (C1) into Eq. (4) we can obtain the Andreev equations [37]

$$\mp i\hbar v_F\frac{\partial}{\partial R}\hat{g}_{E\pm}(\mathbf{r}',R,\mathbf{n}) + \begin{pmatrix} -E & -\Delta(\mathbf{r}) \\ \Delta^*(\mathbf{r}) & E\end{pmatrix}\hat{g}_{E\pm}(\mathbf{r}',R,\mathbf{n}) = 0, \quad \text{(C2)}$$

where $\mathbf{n}$ is a unit vector and $\mathbf{r} = \mathbf{r}' + R\mathbf{n}$. When deriving Eq. (C2) differentiation with respect to the directions of $\mathbf{n}$ has been neglected, which is justified when

$$\frac{\hbar^2}{mR^2|\delta\mathbf{n}|^2} \ll |\Delta|, \quad \text{(C3)}$$

where $\delta\mathbf{n}$ is the characteristic variation scale of $\hat{g}_E^{\pm}(\mathbf{r}',R,\mathbf{n})$ with respect to $\mathbf{n}$. Equation (C3) can be rewritten as

$$|\delta\mathbf{n}|^2 \gg \frac{\xi}{k_F R^2}. \quad \text{(C4)}$$

The uniqueness of the solution of Eq. (C2) is provided by the boundary conditions [37]

$$\hat{g}_{E\pm}(\mathbf{r}',0,\mathbf{n}) = \tfrac{1}{2}[\hat{\tau}_0 \pm \hat{g}_E(\mathbf{r}',\pm\mathbf{n})], \quad \text{(C5)}$$

where $\hat{g}_E(\mathbf{r},\mathbf{n})$ is the conventional quasiclassical Green function, which satisfies the Eilenberger equation [27,28] with the normalization condition $\hat{g}_E^2 = \hat{\tau}_0$.

At small R the condition (C4) is obviously violated. However, a different representation of the Green function may be obtained for $|\mathbf{r}-\mathbf{r}'| \ll \xi$. At such small length scales in the left-hand side of the Gor'kov equation (4) all terms can be neglected except for the kinetic energy. Hence the Green function can be written as

$$\hat{G}_E^{(0)}(\mathbf{r},\mathbf{r}') = \int \hat{g}'_E(\mathbf{r}',\mathbf{n}')e^{ik_F\mathbf{n}'(\mathbf{r}-\mathbf{r}')}d^2\mathbf{n}' + \frac{m}{2\pi\hbar^2}\frac{e^{ik_F|\mathbf{r}-\mathbf{r}'|}}{|\mathbf{r}-\mathbf{r}'|}\hat{\tau}_0, \quad \text{(C6)}$$

where integration goes over a unit sphere and $\hat{g}'_E(\mathbf{r}',\mathbf{n})$ is a function that will be determined shortly. We note that a range of distances $R \ll \xi$ may exist where Eq. (C4) is satisfied. In that range both Eqs. (C1) and (C6) are applicable, and hence should be equivalent to each other. When both $k_F R \gg 1$ and Eq. (C4) are satisfied, the integral in Eq. (C6) can be calculated by the stationary phase method, yielding

$$\hat{G}_E^{(0)}(\mathbf{r},\mathbf{r}') = \frac{e^{ik_F R}}{R}\left[\frac{m}{2\pi\hbar^2} - \frac{2i}{k_F}\hat{g}'_E(\mathbf{r}',\mathbf{n})\right] + \frac{2\pi i e^{-ik_F R}}{k_F R}\hat{g}'_E(\mathbf{r}',-\mathbf{n}). \quad \text{(C7)}$$

Comparing this with Eq. (C1), we find that

$$\hat{g}'_E(\mathbf{r}',\mathbf{n}) = \frac{imk_F}{4\pi^2\hbar^2}[\hat{g}_{E+}(\mathbf{r}',0,\mathbf{n}) - \hat{\tau}_0] = -\frac{imk_F}{4\pi^2\hbar^2}\hat{g}_{E-}(\mathbf{r}',0,-\mathbf{n}). \quad \text{(C8)}$$

Finally, taking into account Eq. (C5), we obtain Eq. (16) [38].

Using the approach outlined above, we will now determine the Green functions $G_E^{(0)}(\mathbf{r},\mathbf{r}')$ and $F_E^{\dagger(0)}(\mathbf{r},\mathbf{r}')$ for a clean short SNS junction (Fig. 2 without the defect). We will assume that the vector $\mathbf{r}'$ lies in the normal layer. For a start, we need the solutions of the Eilenberger equation, which are known [39]:

$$g_E(\mathbf{r}_1,\mathbf{n}) = i\cot\left[\frac{(E+i\epsilon^+)L}{\hbar v_F|n_z|} - \gamma(E+i\epsilon^+) - \frac{\varphi}{2}\mathrm{sgn}(n_z)\right], \quad \text{(C9)}$$

$$f_E^{\dagger}(\mathbf{r}_1,\mathbf{n}) = \frac{i\,\exp\left(\frac{iE(L_2-L_1)}{\hbar V_F n_z}\right)}{\sin\left[\frac{(E+i\epsilon^+)L}{\hbar v_F|n_z|} - \gamma(E+i\epsilon^+) - \frac{\varphi}{2}\mathrm{sgn}(n_z)\right]}, \quad \text{(C10)}$$

where $\gamma(E)$ is given by Eq. (20). We can put here $\gamma(E+i\epsilon^+)=\gamma(E)$, since the term $i\epsilon^+ L/(\hbar v_F|n_z|)$ in Eqs. (C9) and (C10) already yields the necessary imaginary part in the denominators. Equations (C9) and (C10) are valid for a clean SNS junction of any length, and they allow one to reproduce the long-known zigzag pattern of the density of states [26,40,41].

The Green functions with coinciding arguments are determined using Eq. (16):

$$G_{ER}^{(0)}(\mathbf{r}_1,\mathbf{r}_1)=-\frac{mk_F}{4\pi\hbar^2}\int_{-1}^{1}\cot\left[\frac{EL}{\hbar v_F|n_z|}+i\epsilon^+-\gamma(E)-\frac{\varphi}{2}\mathrm{sgn}(n_z)\right]dn_z, \tag{C11}$$

$$F_E^{\dagger(0)}(\mathbf{r}_1,\mathbf{r}_1)=-\frac{mk_F}{4\pi\hbar^2}\int_{-1}^{1}\frac{\exp\left(\frac{iE(L_2-L_1)}{\hbar V_F n_z}\right)dn_z}{\sin\left[\frac{EL}{\hbar v_F|n_z|}+i\epsilon^+-\gamma(E)-\frac{\varphi}{2}\mathrm{sgn}(n_z)\right]}. \tag{C12}$$

We may note that for most of the directions of the vector $\mathbf{n}$ the ratio $EL/(\hbar v_F|n_z|)$ is small and may be neglected (unless $|n_z|\lesssim|E|L/\hbar v_F$). Doing so, we obtain Eqs. (18) and (19).

When calculating $g_{E\pm}$, for most directions of $\mathbf{n}$ we may additionally disregard the fact that $\Delta(\mathbf{r})=0$ in Eq. (C2) for $R<L_{1,2}/|n_z|$ (as long as $L/|n_z|\ll\xi$). Effectively, this means that we can ignore the normal layer, putting $L=0$. Solving Eq. (C2) with the boundary conditions (C5) then yields

$$g_{E\pm}(\mathbf{r}',R,\mathbf{n})\approx\pm\frac{i\,\exp\left(\pm i\gamma(E)+i\frac{\varphi}{2}\mathrm{sgn}(n_z)-\frac{\sqrt{|\Delta|^2-E^2}}{\hbar v_F}R\right)}{2\,\sin\left(-\gamma(E)\mp\frac{\varphi}{2}\mathrm{sgn}(n_z)\right)}, \tag{C13}$$

$$f_{E\pm}^{\dagger}(\mathbf{r}',R,\mathbf{n})\approx\pm\frac{i\exp\left(-\frac{\sqrt{|\Delta|^2-E^2}}{\hbar v_F}R\right)}{2\,\sin\left(-\gamma(E)\mp\frac{\varphi}{2}\mathrm{sgn}(n_z)\right)}. \tag{C14}$$

Let us substitute this into Eq. (C1):

$$G_E^{(0)}(\mathbf{r},\mathbf{r}')=\frac{mi}{4\pi\hbar^2R}\left[\frac{e^{-ik_FR-i\gamma(E)}}{\sin\left(\gamma(E)-\frac{\varphi}{2}\mathrm{sgn}(n_z)\right)}-\frac{e^{ik_FR+i\gamma(E)}}{\sin\left(\gamma(E)+\frac{\varphi}{2}\mathrm{sgn}(n_z)\right)}\right]\exp\left(i\frac{\varphi}{2}\mathrm{sgn}(n_z)-\frac{\sqrt{|\Delta|^2-E^2}}{\hbar v_F}R\right), \tag{C15}$$

$$F_E^{\dagger(0)}(\mathbf{r},\mathbf{r}')=\frac{mi}{4\pi\hbar^2R}\left[\frac{e^{-ik_FR}}{\sin\left(\gamma(E)-\frac{\varphi}{2}\mathrm{sgn}(n_z)\right)}-\frac{e^{ik_FR}}{\sin\left(\gamma(E)+\frac{\varphi}{2}\mathrm{sgn}(n_z)\right)}\right]\exp\left(-\frac{\sqrt{|\Delta|^2-E^2}}{\hbar v_F}R\right). \tag{C16}$$

These relations are valid for $k_FR\gg1$, $L/|n_z|\ll\xi$, and when Eq. (21) holds. To calculate the Green functions for $R\ll\xi$, we may use Eq. (16) together with Eqs. (C9) and (C10). In the short-junction limit we may again neglect all terms containing L, L_1, and L_2 to obtain

$$G_E^{(0)}(\mathbf{r},\mathbf{r}')\approx\frac{mk_F}{4\pi\hbar^2}\left[K(k_F(\mathbf{r}-\mathbf{r}'))\cot\left(\gamma(E)+\frac{\varphi}{2}\right)+K^*(k_F(\mathbf{r}-\mathbf{r}'))\cot\left(\gamma(E)-\frac{\varphi}{2}\right)\right]+\frac{m\cos(k_F|\mathbf{r}-\mathbf{r}'|)}{2\pi\hbar^2|\mathbf{r}-\mathbf{r}'|}, \tag{C17}$$

$$F_E^{\dagger(0)}(\mathbf{r},\mathbf{r}')\approx\frac{mk_F}{4\pi\hbar^2}\left[K(k_F(\mathbf{r}-\mathbf{r}'))\sin^{-1}\left(\gamma(E)+\frac{\varphi}{2}\right)+K^*(k_F(\mathbf{r}-\mathbf{r}'))\sin^{-1}\left(\gamma(E)-\frac{\varphi}{2}\right)\right], \tag{C18}$$

where

$$K(\mathbf{R})=\int_{n_z>0}e^{i\mathbf{nR}}\frac{d\mathbf{n}}{2\pi}. \tag{C19}$$

Here, integration goes over a unit hemisphere. In the final part of this appendix we will derive some properties of the function $K(\mathbf{R})$.

First, we point out three rather obvious relations:

$$K(0)=1, \tag{C20}$$

$$|K(\mathbf{R})|\leqslant1, \tag{C21}$$

$$K(-\mathbf{R})=K^*(\mathbf{R}). \tag{C22}$$

Now we will transform Eq. (C19). For this, we introduce an auxiliary coordinate frame (x',y,z'), such that the z' axis is directed along the vector $\mathbf{R}$; see Fig. 9. This vector makes an angle β with the z axis, and for now we assume that $\beta\leqslant\pi/2$. Let θ and ϕ be

the polar and azimuthal angles in the (x',y,z') frame, respectively. Then, $n_z = \sin\theta\,\cos\phi\,\sin\beta + \cos\theta\,\cos\beta$. Equation (C19) can be transformed as follows:

$$K(\mathbf{R}) = \iint_{\cos\phi > -\cot\theta\,\cot\beta} \sin\theta e^{iR\,\cos\theta}\frac{d\phi\,d\theta}{2\pi} = \int_0^{\frac{\pi}{2}-\beta} \sin\theta\, e^{iR\,\cos\theta} d\theta + \int_{\frac{\pi}{2}-\beta}^{\frac{\pi}{2}+\beta} \sin\theta\, e^{iR\,\cos\theta}\arccos\left(-\cot\beta\,\cot\theta\right)\frac{d\theta}{\pi}$$
$$= \frac{e^{iR} - e^{iR\,\sin\beta}}{iR} + \int_{-\sin\beta}^{\sin\beta} e^{ixR}\arccos\left(-\frac{x}{\sqrt{1-x^2}}\cot\beta\right)\frac{dx}{\pi}. \tag{C23}$$

After integration by parts we obtain

$$K(\mathbf{R}) = \frac{e^{iR}}{iR} + \frac{i\,\cos\beta}{\pi R}\int_{-\sin\beta}^{\sin\beta}\frac{e^{ixR}dx}{(1-x^2)\sqrt{\sin^2\beta - x^2}} = \frac{e^{iR}}{iR} + \frac{2i\,\cos\beta}{\pi R}\int_0^{\sin\beta}\frac{\cos(xR)dx}{(1-x^2)\sqrt{\sin^2\beta - x^2}}. \tag{C24}$$

It follows from this that

$$\mathrm{Re}[K(\mathbf{R})] = \frac{\sin R}{R}, \tag{C25}$$

$$\mathrm{Im}[K(\mathbf{R})] = \frac{2\,\cos\beta}{\pi R}\int_0^1 \frac{\cos(xR\,\sin\beta)dx}{\sqrt{1-x^2}(1-x^2\sin^2\beta)} - \frac{\cos R}{R}. \tag{C26}$$

Additionally, Eqs. (C22) and (C25) yield

$$K(\mathbf{R}) = \frac{\sin R}{R} \quad \text{when } \beta = \frac{\pi}{2}. \tag{C27}$$

Moreover, there must be $\mathrm{Im}[K(0)] = 0$ [Eq. (C20)], so that

$$\frac{2\,\cos\beta}{\pi}\int_0^1 \frac{dx}{\sqrt{1-x^2}(1-x^2\sin^2\beta)} = 1 \tag{C28}$$

for any $\beta \in [0,\pi/2)$. Using this, we can rewrite Eq. (C26) as

$$\mathrm{Im}[K(\mathbf{R})] = \frac{2\,\cos\beta}{\pi R}\int_0^1 \frac{\cos(xR\,\sin\beta) - \cos R}{\sqrt{1-x^2}(1-x^2\sin^2\beta)}dx. \tag{C29}$$

This relation is also valid for $\beta \in [\pi/2,\pi]$, because the integral is finite and the property (C22) is satisfied. It follows from (C28) and (C29) that

$$|\mathrm{Im}[K(\mathbf{R})]| \leqslant \frac{4|\cos\beta|}{\pi R}\int_0^1 \frac{dx}{\sqrt{1-x^2}(1-x^2\sin^2\beta)} = \frac{2}{R}, \tag{C30}$$

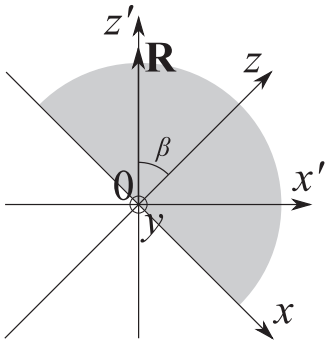

FIG. 9. Coordinate system we use to calculate the function $K(\mathbf{R})$. The unit hemisphere over which we integrate is highlighted in gray.

and hence

$$|K(\mathbf{R})| \leqslant \frac{\sqrt{5}}{R}. \tag{C31}$$

Finally, if we substitute $x = \sin t$ in Eq. (C29), we obtain

$$K(\mathbf{R}) = \frac{\sin R}{R} + \frac{2i\,\cos\beta}{\pi R} \times \int_0^{\pi/2}\frac{\cos(R\,\sin\beta\,\sin t) - \cos R}{1 - \sin^2 t\,\sin^2\beta}dt. \tag{C32}$$

This form is particularly convenient for numerical calculations, because the integrand is a limited and continuous function of β and t. Indeed,

$$\left|\frac{\cos(R\,\sin\beta\,\sin t) - \cos R}{1 - \sin^2 t\,\sin^2\beta}\right| = \frac{R^2}{2}\left|\frac{2\,\sin\left(R\frac{1-\sin\beta\,\sin t}{2}\right)}{R(1-\sin\beta\,\sin t)}\frac{2\,\sin\left(R\frac{1+\sin\beta\,\sin t}{2}\right)}{R(1+\sin\beta\,\sin t)}\right| \leqslant \frac{R^2}{2}. \tag{C33}$$

This relation allows one to obtain another estimate for $\mathrm{Im}[K(\mathbf{R})]$:

$$|\mathrm{Im}[K(\mathbf{R})]| \leqslant \frac{2|\cos\beta|}{\pi R}\int_0^{\pi/2}\frac{R^2}{2}dt = \frac{|R_z|}{2}. \tag{C34}$$

APPENDIX D: IMAGINARY PARTS OF GREEN FUNCTIONS WITH COINCIDING ARGUMENTS

In this Appendix we estimate the imaginary parts of the functions $G^{(0)}_{ER}(\mathbf{r}_1,\mathbf{r}_1)$ and $F^{\dagger(0)}_{E}(\mathbf{r}_1,\mathbf{r}_1)$, given by Eqs. (C11) and (C12), and the width of the impurity resonance, E'_A. The imaginary part of $G^{(0)}_{ER}(\mathbf{r}_1,\mathbf{r}_1)$ originates from the poles of the integrand in Eq. (C11). It can be proven that

$$\mathrm{Im}[\cot(x + i\epsilon^+)] = -\pi\sum_{n=-\infty}^{+\infty}\delta(x - \pi n). \tag{D1}$$

Then

$$\mathrm{Im}\big[G^{(0)}_{ER}(\mathbf{r}_1,\mathbf{r}_1)\big] = \frac{mk_F}{4\hbar^2}\int_{-1}^{1}\sum_{n=-\infty}^{+\infty}\delta\left(\frac{EL}{\hbar v_F|n_z|}+\gamma(E)-\frac{\varphi}{2}\mathrm{sgn}(n_z)\right)dn_z$$
$$= \frac{mk_F|E|L}{4\hbar^3 v_F}\left\{\sum_{\pi n>\frac{|E|L}{\hbar v_F}-\gamma(|E|)-\frac{\varphi}{2}}\left[\gamma(|E|)+\frac{\varphi}{2}+\pi n\right]^{-2}+\sum_{\pi n>\frac{|E|L}{\hbar v_F}-\gamma(|E|)+\frac{\varphi}{2}}\left[\gamma(|E|)-\frac{\varphi}{2}+\pi n\right]^{-2}\right\}. \quad \text{(D2)}$$

It can be seen that when the condition (21) is satisfied, then

$$\mathrm{Im}\big[G^{(0)}_{ER}(\mathbf{r}_1,\mathbf{r}_1)\big] \sim \frac{mk_F|E|L}{4\hbar^3 v_F}. \quad \text{(D3)}$$

The imaginary part of $F^{\dagger(0)}_E(\mathbf{r}_1,\mathbf{r}_1)$ has a similar contribution due to the poles of the integrand in Eq. (C12). In addition, there is generally a larger contribution originating from the exponent in the numerator of the integrand. Applying the Taylor expansion to this exponent, we obtain

$$\mathrm{Im}\big[F^{\dagger(0)}_E(\mathbf{r}_1,\mathbf{r}_1)\big] \approx -\frac{mk_F E(L_2-L_1)}{4\pi\hbar^3 v_F}\left\{\int_{|E|L/\hbar v_F}^{1}\sin^{-1}\left(-\gamma(E)-\frac{\varphi}{2}\right)\frac{dn_z}{n_z}+\int_{-1}^{|E|L/\hbar v_F}\sin^{-1}\left(-\gamma(E)+\frac{\varphi}{2}\right)\frac{dn_z}{n_z}\right\}$$
$$= \frac{mk_F E(L_2-L_1)}{4\pi\hbar^3 v_F}\ln\left(\frac{\hbar v_F}{|E|L}\right)\left[\frac{1}{\sin\left(\gamma(E)+\frac{\varphi}{2}\right)}-\frac{1}{\sin\left(\gamma(E)-\frac{\varphi}{2}\right)}\right], \quad \text{(D4)}$$

assuming that Eq. (21) holds, and $L_2 - L_1 \sim L$. Thus

$$\mathrm{Im}\big[F^{\dagger(0)}_E(\mathbf{r}_1,\mathbf{r}_1)\big] \sim \frac{mk_F|E|L}{4\pi\hbar^3 v_F}\ln\left(\frac{\hbar v_F}{|E|L}\right). \quad \text{(D5)}$$

Now we will estimate the width of the impurity resonance, E'_A. First, we note that at real energies the imaginary part of the determinant $\mathcal{D}_\uparrow$ [Eq. (15)] equals

$$\mathrm{Im}[\mathcal{D}_\uparrow] = -2\,\mathrm{Im}\big[G^{(0)}_{ER}(\mathbf{r}_1,\mathbf{r}_1)\big]\mathrm{Re}\big[G^{(0)}_{ER}(\mathbf{r}_1,\mathbf{r}_1)\big]$$
$$-\mathrm{Re}\big[F^{\dagger(0)}_E(\mathbf{r}_1,\mathbf{r}_1)\big]\mathrm{Im}\big[F^{\dagger(0)}_{-E}(\mathbf{r}_1,\mathbf{r}_1)\big]$$
$$+\mathrm{Re}\big[F^{\dagger(0)}_{-E}(\mathbf{r}_1,\mathbf{r}_1)\big]\mathrm{Im}\big[F^{\dagger(0)}_{E}(\mathbf{r}_1,\mathbf{r}_1)\big]. \quad \text{(D6)}$$

According to Eqs. (D3) and (D5), the first line of Eq. (D6) is generally much smaller than the second and third lines; however, the latter two lines almost cancel each other out, as follows from Eqs. (19) and (D5). Hence

$$\mathrm{Im}[\mathcal{D}_\uparrow] \sim 2\,\mathrm{Im}\big[G^{(0)}_{ER}(\mathbf{r}_1,\mathbf{r}_1)\big]\mathrm{Re}\big[G^{(0)}_{ER}(\mathbf{r}_1,\mathbf{r}_1)\big]$$
$$\sim \frac{m^2k_F^2}{\hbar^4}\frac{|E|L}{\hbar v_F}, \quad \text{(D7)}$$

as long as Eq. (21) holds. For a complex energy $E = E_A - iE'_A$ with a small imaginary part we have

$$\mathrm{Im}[\mathcal{D}_\uparrow(E_A - iE'_A)] \approx \mathrm{Im}[\mathcal{D}_\uparrow(E_A)] - E'_A\frac{\partial\mathcal{D}_\uparrow}{\partial E}(E_A), \quad \text{(D8)}$$

where $\partial\mathcal{D}_\uparrow/\partial E$ is determined using Eq. (22). Equating $\mathrm{Im}[\mathcal{D}_\uparrow]$ to zero, we obtain Eq. (24).

APPENDIX E: ELECTRON TRANSMISSION THROUGH A NORMAL LAYER WITH TWO IMPURITIES

In this Appendix we calculate the eigenvalues of the matrix $\hat{T} = \hat{t}\hat{t}^\dagger$ for the N layer with two impurities—see Fig. 7. First, the transmission matrix $\hat{t}$ should be determined. For this, we define a set of propagating electron modes in the N layer. To obtain a finite set of such modes, we apply periodic boundary conditions in the xy plane. Then, the orthogonal wave functions of electrons propagating from left to right through a clean N layer are

$$\psi^{(0)}_n(\mathbf{r}) = \sqrt{\frac{m}{\hbar^2 k_{nz}S_\perp}}e^{i\mathbf{k}_n\mathbf{r}}, \quad \text{(E1)}$$

where $k_{nz} > 0$, $|\mathbf{k}_n| = k_F$, and $S_\perp$ is the cross section of the N layer. The allowed values of the wave vectors $\mathbf{k}_n$ are determined by the boundary conditions in the xy plane. Note that for calculations of scattering matrices we need to normalize the wave functions so that they carry a unit total current:

$$-S_\perp\frac{\hbar^2 i}{2m}\left(\psi^{(0)*}_n\frac{\partial\psi^{(0)}_n}{\partial z}-\psi^{(0)}_n\frac{\partial\psi^{(0)*}_n}{\partial z}\right) = 1. \quad \text{(E2)}$$

In the presence of impurities electrons are scattered, so that their wave functions become

$$\psi_n(\mathbf{r}) = \sqrt{\frac{m}{\hbar^2 k_{nz}S_\perp}}\left(e^{i\mathbf{k}_n\mathbf{r}}+\frac{A_1e^{ik_Fr}}{k_Fr}+\frac{A_2e^{ik_F|\mathbf{r}-\mathbf{r}_2|}}{k_F|\mathbf{r}-\mathbf{r}_2|}\right). \quad \text{(E3)}$$

The amplitudes A_1 and A_2 are determined from Eqs. (B3) and (B5) (with the Green function replaced by the wave function) applied to each impurity. This yields [42]

$$A_1 = \mathcal{D}_2^{-1}e^{i\alpha_1}\sin\alpha_1\left(1+\frac{e^{ik_Fr_2+i\alpha_2+i\mathbf{k}_n\mathbf{r}_2}\sin\alpha_2}{k_Fr_2}\right), \quad \text{(E4)}$$

$$A_2 = \mathcal{D}_2^{-1}e^{i\alpha_2}\sin\alpha_2\left(e^{i\mathbf{k}_n\mathbf{r}_2}+\frac{e^{ik_Fr_2+i\alpha_1}\sin\alpha_1}{k_Fr_2}\right), \quad \text{(E5)}$$

$$\mathcal{D}_2 = 1-\frac{e^{2ik_Fr_2+i\alpha_1+i\alpha_2}}{k_F^2r_2^2}\sin\alpha_1\sin\alpha_2. \quad \text{(E6)}$$

The transmission matrix is defined as follows:

$$t_{n'n} = \frac{\iint_{S_\perp} \psi_n(x,y,Z)\psi^{(0)*}_{n'}(x,y,Z)dx\,dy}{\iint_{S_\perp} \left|\psi^{(0)}_{n'}(x,y,Z)\right|^2 dx\,dy}, \tag{E7}$$

where Z is any number larger than z_2. Here, the numerator contains two integrals of the form

$$I = \iint_{S_\perp} \frac{e^{ik_F|\mathbf{r}-\mathbf{r}_i|}}{|\mathbf{r}-\mathbf{r}_i|} e^{-i\mathbf{k}_{n'}\mathbf{r}}\Big|_{z=Z} dx\,dy, \tag{E8}$$

where $\mathbf{r}_i = 0$ or $\mathbf{r}_i = \mathbf{r}_2$, and we will denote the components of $\mathbf{r}_i$ as (x_i, y_i, z_i). To evaluate the integral in Eq. (E8), we first make an inverse Fourier transform:

$$\frac{e^{ik_F|\mathbf{r}-\mathbf{r}_i|}}{|\mathbf{r}-\mathbf{r}_i|} = \int \frac{e^{i\mathbf{q}(\mathbf{r}-\mathbf{r}_i)}}{q^2 - k_F^2 - i\epsilon^+} \frac{d^3\mathbf{q}}{2\pi^2}. \tag{E9}$$

Using this, integration over x and y in Eq. (E8) becomes straightforward, and after that integration over q_x and q_y can be performed. We have then

$$\begin{aligned} I &= 2\,\exp(-ik_{n'z}Z - ik_{n'x}x_i - ik_{n'y}y_i)\int_{-\infty}^{+\infty} \frac{e^{iq_z(Z-z_i)}dq_z}{q_z^2 - k_{n'z}^2 - i\epsilon^+} \\ &= 4\pi i\,\exp(-ik_{n'z}Z - ik_{n'x}x_i - ik_{n'y}y_i)\operatorname*{Res}_{q_z=k_{n'z}} \frac{e^{iq_z(Z-z_i)}}{q_z^2 - k_{n'z}^2} = 2\pi i k_{n'z}^{-1} e^{-i\mathbf{k}_{n'}\mathbf{r}_i}. \end{aligned} \tag{E10}$$

This relation allows one to obtain

$$t_{n'n} = \delta_{n'n} + \frac{2\pi i \mathcal{D}_2^{-1} S_\perp^{-1}}{\sqrt{k_{nz}k_{n'z}}k_F}\left[e^{i\alpha_1}\sin\alpha_1\left(1 + \frac{e^{ik_Fr_2 + i\alpha_2 + i\mathbf{k}_n\mathbf{r}_2}\sin\alpha_2}{k_Fr_2}\right) + e^{i\alpha_2 - i\mathbf{k}_{n'}\mathbf{r}_2}\sin\alpha_2\left(e^{i\mathbf{k}_n\mathbf{r}_2} + \frac{e^{ik_Fr_2+i\alpha_1}\sin\alpha_1}{k_Fr_2}\right)\right]. \tag{E11}$$

The Hermitian conjugate to this matrix is defined in the usual way: $t^\dagger_{n'n} = t^*_{nn'}$. It can be seen that $\hat{t}$ and $\hat{t}^\dagger$ have a common invariant subspace $\mathcal{W}$, which is spanned by the vectors $\boldsymbol{\rho}$ and $\boldsymbol{\nu}$ with components

$$\rho_n = \left(\frac{2\pi}{k_{nz}k_FS_\perp}\right)^{1/2}, \quad \nu_n = \left(\frac{2\pi}{k_{nz}k_FS_\perp}\right)^{1/2} e^{-i\mathbf{k}_n\mathbf{r}_2}. \tag{E12}$$

In the orthogonal complement of $\mathcal{W}$ the operators $\hat{t}$ and $\hat{t}^\dagger$ act as identity operators. Hence the eigenvectors of $\hat{T}$ corresponding to nonunit eigenvalues lie in the subspace $\mathcal{W}$. In the basis $\{\boldsymbol{\rho}, \boldsymbol{\nu}\}$ the operators $\hat{t}$ and $\hat{t}^\dagger$ have the matrices $\hat{t}'$ and $\hat{t}^{\dagger\prime}$, respectively:

$$\begin{pmatrix}\hat{t}\boldsymbol{\rho}\\ \hat{t}\boldsymbol{\sigma}\end{pmatrix} = \begin{pmatrix}t'_{11} & t'_{12}\\ t'_{21} & t'_{22}\end{pmatrix}\begin{pmatrix}\boldsymbol{\rho}\\ \boldsymbol{\sigma}\end{pmatrix}, \quad \begin{pmatrix}\hat{t}^\dagger\boldsymbol{\rho}\\ \hat{t}^\dagger\boldsymbol{\sigma}\end{pmatrix} = \begin{pmatrix}t^{\dagger\prime}_{11} & t^{\dagger\prime}_{12}\\ t^{\dagger\prime}_{21} & t^{\dagger\prime}_{22}\end{pmatrix}\begin{pmatrix}\boldsymbol{\rho}\\ \boldsymbol{\sigma}\end{pmatrix}, \tag{E13}$$

Here, we will illustrate how to calculate one of the components of these matrices. By definition, $\hat{t}\boldsymbol{\rho} = t'_{11}\boldsymbol{\rho} + t'_{21}\boldsymbol{\sigma}$; hence

$$\begin{aligned} t'_{11} &= 1 + \sum_n \frac{2\pi i e^{i\alpha_1}\sin\alpha_1}{k_{nz}k_FS_\perp\mathcal{D}_2}\left(1 + \frac{e^{ik_Fr_2+i\alpha_2+i\mathbf{k}_n\mathbf{r}_2}\sin\alpha_2}{k_Fr_2}\right) \\ &= 1 + \frac{ie^{i\alpha_1}\sin\alpha_1}{\mathcal{D}_2}\iint_{k_\perp<k_F}\left(1 + \frac{e^{ik_Fr_2+i\alpha_2+i\mathbf{k}\mathbf{r}_2}\sin\alpha_2}{k_Fr_2}\right)\frac{d^2\mathbf{k}_\perp}{2\pi k_zk_F}, \end{aligned} \tag{E14}$$

where $\mathbf{k}_\perp$ is the perpendicular to the z axis component of $\mathbf{k}$ and $k_z = \sqrt{k_F^2 - k_\perp^2}$. To obtain the second line of Eq. (E14), we went from summation to integration using the common substitution

$$\sum_n \to \frac{S_\perp}{(2\pi)^2}\int d^2\mathbf{k}_\perp.$$

Introducing the unit vector $\mathbf{n} = \mathbf{k}/k_F$, we can rewrite Eq. (E14) in the form

$$t'_{11} = 1 + \frac{ie^{i\alpha_1}\sin\alpha_1}{\mathcal{D}_2}\int_{n_z>0}\left(1 + \frac{e^{ik_Fr_2+i\alpha_2+ik_F\mathbf{n}\mathbf{r}_2}\sin\alpha_2}{k_Fr_2}\right)\frac{d^2\mathbf{n}}{2\pi} = 1 + \frac{ie^{i\alpha_1}}{\mathcal{D}_2}\sin\alpha_1\left[1 + \frac{e^{i\alpha_2+ik_Fr_2}\sin\alpha_2}{k_Fr_2}K(k_F\mathbf{r}_2)\right]. \tag{E15}$$

All other components of $\hat{t}'$ and $\hat{t}^{\dagger\prime}$ can be calculated in a similar way, and the result is

$$\hat{t}' = \begin{pmatrix} 1 + \frac{ie^{i\alpha_1}}{\mathcal{D}_2}\sin\alpha_1\left[1 + \frac{e^{i\alpha_2+ik_Fr_2}\sin\alpha_2}{k_Fr_2}K(k_F\mathbf{r}_2)\right] & \frac{ie^{i\alpha_1}}{\mathcal{D}_2}\sin\alpha_1\left[K^*(k_F\mathbf{r}_2) + \frac{e^{i\alpha_2+ik_Fr_2}\sin\alpha_2}{k_Fr_2}\right] \\ \frac{ie^{i\alpha_2}}{\mathcal{D}_2}\sin\alpha_2\left[K(k_F\mathbf{r}_2) + \frac{e^{i\alpha_1+ik_Fr_2}\sin\alpha_1}{k_Fr_2}\right] & 1 + \frac{ie^{i\alpha_2}}{\mathcal{D}_2}\sin\alpha_2\left[1 + \frac{e^{i\alpha_1+ik_Fr_2}\sin\alpha_1}{k_Fr_2}K^*(k_F\mathbf{r}_2)\right] \end{pmatrix}, \tag{E16}$$

$$\hat{t}^{\dagger\prime} = \begin{pmatrix} 1 - \frac{ie^{-i\alpha_1}}{\mathcal{D}_2^*}\sin\alpha_1\left[1 + \frac{e^{-i\alpha_2 - ik_F r_2}\sin\alpha_2}{k_F r_2}K(k_F\mathbf{r}_2)\right] & -\frac{ie^{-i\alpha_1}}{\mathcal{D}_2^*}\sin\alpha_1\left[K^*(k_F\mathbf{r}_2) + \frac{e^{-i\alpha_2 - ik_F r_2}\sin\alpha_2}{k_F r_2}\right] \\ \frac{-ie^{-i\alpha_2}}{\mathcal{D}_2^*}\sin\alpha_2\left[K(k_F\mathbf{r}_2) + \frac{e^{-i\alpha_1 - ik_F r_2}\sin\alpha_1}{k_F r_2}\right] & 1 - \frac{ie^{-i\alpha_2}}{\mathcal{D}_2^*}\sin\alpha_2\left[1 + \frac{e^{-i\alpha_1 - ik_F r_2}\sin\alpha_1}{k_F r_2}K^*(k_F\mathbf{r}_2)\right] \end{pmatrix}. \tag{E17}$$

Note that $t'^{\dagger\prime}_{n'n} \neq t'^{*}_{nn'}$, because the vectors $\boldsymbol{\rho}$ and $\boldsymbol{\sigma}$ are not orthogonal.

The nonunit eigenvalues of the matrix $\hat{T}$ are determined by the equation $\det(\hat{t}'\hat{t}^{\dagger\prime} - \hat{1}T_i) = 0$, or

$$T_i^2 - \mathrm{Tr}(\hat{t}'\hat{t}^{\dagger\prime})T_i + \det(\hat{t}'\hat{t}^{\dagger\prime}) = 0. \tag{E18}$$

The solution of this equation is

$$T_{1,2} = \frac{\mathrm{Tr}(\hat{t}'\hat{t}^{\dagger\prime}) \pm \sqrt{[\mathrm{Tr}(\hat{t}'\hat{t}^{\dagger\prime})]^2 - 4\det(\hat{t}'\hat{t}^{\dagger\prime})}}{2}. \tag{E19}$$

Below we will analyze the behavior of T_1 and T_2 in several interesting cases. First, let the impurities be very close to each other: $k_F r_2 \ll 1$. Then, they can be roughly described as one impurity with some scattering phase α_0. Indeed, for $r \gg r_2$ Eq. (E3) takes the form

$$\psi_n(\mathbf{r}) \approx \frac{1}{\sqrt{k_{nz}S_\perp}}\left(e^{i\mathbf{k}_n\mathbf{r}} + \frac{\exp\left(ik_F\left|\mathbf{r} - \frac{\mathbf{r}_2}{2}\right| + i\alpha_0\right)}{k_F\left|\mathbf{r} - \frac{\mathbf{r}_2}{2}\right|}\sin\alpha_0\right), \tag{E20}$$

with

$$e^{i\alpha_0}\sin\alpha_0 = (\cot\alpha_0 - i)^{-1} \approx (A_1 + A_2)\exp\left(\frac{-i\mathbf{k}_n\mathbf{r}_2}{2}\right). \tag{E21}$$

Using the Taylor expansion of $\exp(ik_F r_2)$, we obtain from Eqs. (E4)–(E6) and (E21) that

$$\tan\alpha_0 = \frac{\sin(\alpha_1 + \alpha_2) + \frac{2\sin\alpha_1\sin\alpha_2}{k_F r_2}}{\cos(\alpha_1 - \alpha_2) - \frac{\sin\alpha_1\sin\alpha_2}{k_F^2 r_2^2}}. \tag{E22}$$

It turns out that α_0 is a nontrivial function of α_1, α_2, and r_2. When $k_F r_2 \ll |\sin\alpha_1\sin\alpha_2|$, Eq. (E22) yields $\alpha_0 \approx -2k_F r_2$—the resulting scattering phase is small and does not depend on α_1 and α_2. In the opposite limit, $k_F^2 r_2^2 \gg |\sin\alpha_1\sin\alpha_2|$, we have $\alpha_0 \approx \alpha_1 + \alpha_2$. On the other hand, when

$$|\alpha_1|, |\alpha_2| \ll 1, \quad \alpha_1\alpha_2 \approx k_F^2 r_2^2, \tag{E23}$$

we obtain $\alpha_0 \approx \pi/2$, even though both α_1 and α_2 are small. When Eq. (E23) is satisfied, the determinant $\mathcal{D}_2$ is small. This corresponds to a resonant state, which is present even in a system without superconductivity.

The fact that we effectively have one point defect in the limit $k_F r_2 \ll 1$ means that only one mode in the N layer is affected by disorder, which results in $T_1 \approx 1$ and $T_2 \approx \cos^2\alpha_0$.

Let us now place the impurities sufficiently far apart from each other, so that $k_F r_2 \gtrsim 1$. Then, T_1 and T_2 are oscillating functions of both r_2 and β, as can be seen in Fig. 8. Remarkably, the period and amplitude of the oscillations in the T_1 and T_2 vs r_2 dependencies may strongly depend on β, as demonstrated in Figs. 8(c) and 8(d).

In the limit $k_F r_2 \gg 1$ we expect the two impurities to act independently, so that $T_1 \approx \cos^2\alpha_1$ and $T_2 \approx \cos^2\alpha_2$ when $|\alpha_1| \geqslant |\alpha_2|$. Indeed, from Eqs. (E16) and (E17) we obtain

$$\det(\hat{t}'\hat{t}^{\dagger\prime}) = \cos^2\alpha_1\cos^2\alpha_2 + O\left(\frac{1}{k_F^2 r_2^2}\right), \tag{E24}$$

$$\mathrm{Tr}(\hat{t}'\hat{t}^{\dagger\prime}) = \cos^2\alpha_1 + \cos^2\alpha_2 + O\left(\frac{1}{k_F^2 r_2^2}\right), \tag{E25}$$

so that

$$T_1 = \cos^2\alpha_1 + O\left(\frac{1}{k_F^2 r_2^2}\right), \quad T_2 = \cos^2\alpha_2 + O\left(\frac{1}{k_F^2 r_2^2}\right) \tag{E26}$$

when $|\alpha_1| \neq |\alpha_2|$, and

$$T_1 = \cos^2\alpha_1 + O\left(\frac{1}{k_F r_2}\right), \quad T_2 = \cos^2\alpha_1 + O\left(\frac{1}{k_F r_2}\right) \tag{E27}$$

when $|\alpha_1| = |\alpha_2|$. In any case, $k_F r_2 \gg 1$ results in $|T_{1,2} - \cos^2\alpha_{1,2}| \ll 1$.

Finally, we would like to point out a curious observation: when exactly $\alpha_1 = \alpha_2 = -k_F r_2$, the two transmission values T_1 and T_2 coincide and are equal to

$$T_{1,2} = 1 - \frac{\sin^2(k_F r_2)}{1 - \frac{\sin^2(k_F r_2)}{k_F^2 r_2^2}}[1 - |K(k_F\mathbf{r}_2)|^2]. \tag{E28}$$

[1] P. Anderson, J. Phys. Chem. Solids **11**, 26 (1959).
[2] A. A. Abrikosov and L. P. Gor'kov, Sov. Phys. JETP **12**, 1243 (1961).
[3] A. V. Balatsky, I. Vekhter, and J.-X. Zhu, Rev. Mod. Phys. **78**, 373 (2006).
[4] *Mesoscopic Phenomena in Solids*, edited by B. L. Altshuler, P. A. Lee, and W. R. Webb, Modern Problems in Condensed Matter Sciences (Elsevier Science Publishers B.V., North-Holland, Amsterdam, 1991).
[5] J. Friedel, Philos. Mag. **43**, 153 (1952).
[6] L. Yu, Acta Phys. Sin. **21**, 75 (1965).
[7] H. Shiba, Prog. Theor. Phys. **40**, 435 (1968).
[8] A. I. Rusinov, Sov. Phys. JETP **29**, 1101 (1969) [Zh. Eksp. Teor. Fiz. **56**, 2047 (1969)].
[9] A. I. Larkin and Y. N. Ovchinnikov, Phys. Rev. B **57**, 5457 (1998).
[10] A. A. Koulakov and A. I. Larkin, Phys. Rev. B **59**, 12021 (1999).
[11] A. A. Koulakov and A. I. Larkin, Phys. Rev. B **60**, 14597 (1999).

[12] A. A. Golubov, M. Y. Kupriyanov, and E. Il'ichev, Rev. Mod. Phys. **76**, 411 (2004).
[13] M. Eschrig, arXiv:1509.07818 [cond-mat.supr-con].
[14] A. D. Zaikin and G. Zharkov, Sov. Phys. JETP **51**, 364 (1980) [Zh. Eksp. Teor. Fiz **78**, 721 (1980)].
[15] M. Hurd, S. Datta, and P. F. Bagwell, Phys. Rev. B **56**, 11232 (1997).
[16] G. A. Gogadze, Low Temp. Phys. **24**, 685 (1998).
[17] I. Petković, N. M. Chtchelkatchev, and Z. Radović, Phys. Rev. B **73**, 184510 (2006).
[18] V. Paltoglou, I. Margaris, and N. Flytzanis, J. Phys. A **41**, 455301 (2008).
[19] B. Kastening, D. K. Morr, L. Alff, and K. Bennemann, Phys. Rev. B **79**, 144508 (2009).
[20] M. S. Kalenkov, A. V. Galaktionov, and A. D. Zaikin, Phys. Rev. B **79**, 014521 (2009).
[21] G. Annunziata, H. Enoksen, J. Linder, M. Cuoco, C. Noce, and A. Sudbø, Phys. Rev. B **83**, 144520 (2011).
[22] L. Covaci, F. M. Peeters, and M. Berciu, Phys. Rev. Lett. **105**, 167006 (2010).
[23] W. A. Muñoz, L. Covaci, and F. M. Peeters, Phys. Rev. B **91**, 054506 (2015).
[24] Y. S. Avotina, Y. A. Kolesnichenko, and J. M. van Ruitenbeek, Low Temp. Phys. **34**, 936 (2008).
[25] A. N. Omelyanchouk, R. de Bruyn Ouboter, and C. J. Muller, Low Temp. Phys. **20**, 398 (1994) [Fiz. Nizk. Temp. **20**, 501 (1994)].
[26] C. Ishii, Prog. Theor. Phys. **47**, 1464 (1972).
[27] N. Kopnin, *Theory of Nonequilibrium Superconductivity*, International Series of Monographs on Physics (Clarendon Press, Oxford, 2001).
[28] G. Eilenberger, Z. Phys. A: Hadrons Nucl. **214**, 195 (1968).
[29] K. K. Likharev, Rev. Mod. Phys. **51**, 101 (1979).
[30] Y. S. Barash and I. V. Bobkova, Phys. Rev. B **65**, 144502 (2002).
[31] C. W. J. Beenakker, Phys. Rev. Lett. **67**, 3836 (1991).
[32] Ø. Fischer, M. Kugler, I. Maggio-Aprile, C. Berthod, and C. Renner, Rev. Mod. Phys. **79**, 353 (2007).
[33] G. C. Menard, S. Guissart, C. Brun, S. Pons, V. S. Stolyarov, F. Debontridder, M. V. Leclerc, E. Janod, L. Cario, D. Roditchev, P. Simon, and T. Cren, Nat. Phys. **11**, 1013 (2015).
[34] M. Büttiker, Y. Imry, R. Landauer, and S. Pinhas, Phys. Rev. B **31**, 6207 (1985).
[35] A. Albeverio, F. Gesztesy, R. Høegh-Krohn, and H. Holden, *Solvable Models in Quantum Mechanics* (AMS Chelsea Publishing, Providence, RI, 2005).
[36] L. Landau and E. Lifshits, *Quantum Mechanics: Non-relativistic Theory* (Butterworth-Heinemann, Oxford, 1977).
[37] L. P. Gor'kov and N. B. Kopnin, Sov. Phys. JETP **37**, 183 (1973) [Zh. Eksp. Teor. Fiz **64**, 356 (1973)].
[38] An alternative way to derive Eq. 16 is by applying the definition of the quasiclassical Green functions (as described in Ref. [27]) to Eq. (C3). This directly gives a connection between $\hat{g}'_E(r,n)$ and $\hat{g}_E(r,n)$.
[39] A. V. Svidzinskii, *Space-Inhomogeneous Problems in the Theory of Superconductivity* (Nauka, Moscow, 1982).
[40] P. de Gennes and D. Saint-James, Phys. Lett. **4**, 151 (1963).
[41] D. Saint-James, J. Phys. (France) **25**, 899 (1964).
[42] A solution of a more general problem of scattering by an arbitrary number of point scatterers can be found, e.g., in Ref. [35].